PHYSICAL REVIEW D **90,** 054001 (2014)

Higher hybrid charmonia in an extended potential model

M. Atif Sultan,[1,*] Nosheen Akbar,[2,†] Bilal Masud,[1,‡] and Faisal Akram[1,§]

[1]*Centre For High Energy Physics, University of the Punjab, Lahore 54590, Pakistan*

[2]*COMSATS Institute of Information and Technology, Lahore 54000, Pakistan*

(Received 1 April 2014; revised manuscript received 19 July 2014; published 3 September 2014)

The quark potential model for mesons and its extension for hybrid mesons are used to study the effects of radial excitations on the masses, sizes, and radial wave functions at the origin for conventional and hybrid charmonium mesons. These nonrelativistic quark potential models are also used to calculate the $E1$ and $M1$ radiative partial widths for conventional meson to meson and hybrid to hybrid transitions. Relativistic corrections in masses and radiative widths are calculated by applying leading-order perturbation theory. To numerically solve the required Schrödinger equation for the radial wave functions, to be relativistically improved, we use the shooting method. We compare our results with the experimentally observed and theoretically predicted results of the other models. Our results have implications for scalar form factors, energy shifts, and polarizabilities of conventional and hybrid mesons. The comparison of masses of conventional and hybrid charmonium mesons with the masses of recently discovered XYZ particles is also discussed. Thus, our results can help in experimentally recognizing hybrid mesons.

DOI: 10.1103/PhysRevD.90.054001 PACS numbers: 14.40.Lb, 14.40.Pq, 12.39.Pn

I. INTRODUCTION

In conditions where the established theory of hadronic physics, namely, quantum chromodynamics (QCD), cannot be solved, we use a variety of models to explain the hadronic properties. To test these models, we can compare them with numerical simulations of QCD, like those through the lattice gauge theory, and available results of hard experiments. (The effort remains to use these discrete tests of continuum models for improvements in the models so as to get better agreements in the next comparisons. This is an important route of advancing our understanding of the hadronic physics and QCD.) Such hard experiments could be cross sections, decay rates, masses, and J^{PC} (angular momentum, parity, and C parity) combinations of hadrons. In this paper, we present a comprehensive list of phenomenological implications in the charmonium sector, in the form of masses, radii, and wave functions at origin for a variety of J^{PC} assignments, of a model previously proposed [1] by us for hybrid mesons. This model is an extension of the quark potential model to incorporate the knowledge of the gluonic excitations provided by lattice gauge theory; this analytic model was noted to have a very good agreement with the corresponding lattice gauge theory based numerical results. If this QCD-motivated model can explain properties of newly discovered mesons, including many hybrid candidates, this should be a useful advancement in our understanding of the gluonic excitations and, in general, of the physics beyond the quark model. In our quest for comprehensiveness, we address the radial and orbital excitations along with the previously worked out [1] radially ground state gluonic excitations (hybrids) and, while incorporating the relativistic effects as well, try to explain the properties of the newly discovered mesons mentioned below in the charmonium sector.

In general, an important guide to the search of physics beyond the quark model is the set of meson J^{PC} combinations like $0^{--}, 0^{+-}, 1^{-+}, 2^{+-}$, and 3^{-+} [2] not satisfying the quark model formulas $P = (-1)^{L+1}$ and $C = (-1)^{L+S}$. Among the theoretical options to understand such exotic mesons, hybrid is an important option with some expected features often predicted through the existing models of hybrids or numerical simulations of the excited gluonic field in QCD. Guided by theoretical signatures for hybrids, it is not uncommon to find experimentalists specifically searching for hybrid mesons: CERN COMPASS has been [3] centered on hybrid meson structure studies, along with pion polarizability. Progress on this project is reported, for example, in Ref. [4]. Hybrid interpretations of some results from B factories have been discussed in Ref. [5]. Reference [6] then discussed available experimental evidence for exotic hybrid mesons and described the GlueX experiment in Hall D of the Jefferson Laboratory as a new initiative for performing detailed spectroscopy of the light-quark meson spectrum. This collaboration aims to investigate the full spectrum of mesonic states up to roughly 3 GeV, including hybrid candidates; the photoproduction in it promises to be rich in hybrids, starting with those having exotic quantum numbers. Hence, this experiment has been expected to provide detailed spectroscopy necessary to map out the hybrid meson spectrum, which is essential for an understanding of the confinement mechanism and the nature of the gluon in QCD. This primary motivation of

*atifsultan.pu@gmail.com
†nosheenakbar@ciitlahore.edu.pk; noshinakbar@yahoo.com
‡bilalmasud.chep@pu.edu.pk
§faisal.chep@pu.edu.pk

GlueX has been restated in more recent proposals [7], so as to search for and ultimately study the pattern of gluonic excitations in the meson spectrum produced in γp collisions. The spectroscopic searches for the exotic hybrid states such as the $cg\bar{c}$ system in the CLEO-c Research Program [8]. The PANDA (antiproton annihilation at Darmstadt) experiment features a scientific program devoted [9] to charmonium spectroscopy and gluonic excitations (hybrids, glueballs), along with some other topics. This experiment performs studies of the strong interaction via precision spectroscopy of charmonium and open-charm states, an extensive search for exotic objects such as glueballs and hybrids, in-medium and hypernuclei spectroscopy, and more. Reference [10] says "The research of charmonium and charmed hybrids using the antiproton beam with momentum ranging from 1 GeV/c to 15 GeV/c in PANDA experiment at FAIR is perspective and interesting from the scientific point of view. Charmonium and charmed hybrids with different quantum numbers are copiously produced in antiproton-proton annihilation process." Reference [11] says that for the PANDA experiment, "Its set-up allows physicists to address questions like the structure of glueballs and hybrids, to clarify the nature of the X, Y, and Z states," and other related ones. This also tells us that the Crystal Barrel Collaboration searched for hybrids with the exotic quantum numbers $J^{PC} = 1^{-+}$.

Many exotic mesons are suggested to be hybrids. For example, Ref. [12] mentions three experimental candidates for a light 1^{-+} hybrid: $\pi_1(1400)$, observed by E852, VES, and the Crystal Barrel experiment; $\pi_1(1600)$, observed by E852 and VES; and $\pi_1(2000)$, observed by E852; see also Ref. [13] for the latter two mesons, which also describes $\pi_2(1880)$ as a hybrid meson candidate. Reference [14] proposes that a structure at 2175 MeV observed by the *BABAR* Collaboration is a 1^{--} strangeonium hybrid. The first paper of Ref. [5] and Refs. [15,16] interpret $Y(4260)$ as a $c\bar{c}g$ hybrid. Among the possible interpretations of the recently discovered XYZ mesons, the hybrid option is commonly advocated; see Refs. [17,18].

As mentioned above, it is because of the theoretical work on hybrids that we know how to interpret an exotic meson as a hybrid. Thus, it is crucial to improve this type of work both in terms of improved predictions of the existing models and taking models closer to QCD as much as this is known. Available studies include those through the flux-tube model [14,19–24], the QCD string model [25,26], the quark model with a constituent gluon [27–29], the lattice QCD [30–43], and the QCD sum rules [44–49], using a many-body Coulomb gauge Hamiltonian [50–55].

The charmonium system is very significant both for testing models of QCD and our understanding of QCD effects as well as interpreting the recent meson spectrum. For example, Barnes says [2] that the "charmonium system is an excellent laboratory for studying nonperturbative effects such as confinement and gluonic excitations" and "identification of complete hybrid multiplet, especially J^{PC} exotics, would be a crucial contribution to our understanding of the dynamics of gluonic excitations." Ketzer says in Ref. [56] "To avoid experimental difficulties in the light quark sector due to the high density of ordinary $q\bar{q}$ states below 2.5 GeV/c^2, a search for hybrids in the less populated charmonium mass region is expected to be very rewarding." This opinion is reiterated by many others working on hybrids; see, for example, Refs. [5,15–18,25,28,32,33,35–40,43–45,47,48,50,52].

A possible approach to take advantage of all the theoretical approaches to understand hybrid mesons is to use the numbers generated by lattice simulations of QCD (for discretized configurations of quarks and antiquarks) to constrain the form and parameters of a continuum model that is motivated directly or indirectly by QCD. Once that is done, we can compare the model with the results of actual hard experiments. The phenomenological implications we report result from fitting to the lattice results an explicitly written extension of the quark potential $V_{q\bar{q}}(\mathbf{r})$ whose use is *not* limited to finding properties of the ground state hybrid mesons; $(\mathbf{r})$ is the relative vector, a quark and an antiquark. Like any potential model, the relation of the model to QCD can perhaps be most easily seen through what is termed the Born-Oppenheimer approach already used in hadronic physics in Ref. [53] and later in Refs. [1,54]: taking energy of the quickly adjusting gluonic field, found through the numerical lattice simulations of QCD, to be our adiabatic quark-antiquark potential $V_{q\bar{q}}(\mathbf{r})$, we first fit its parameters. Then, we solve the resulting Schrödinger equation for a set of possible quantum numbers of quark-antiquark pairs to calculate the resulting meson energies and wave functions; for hybrids, we used the additional term [1] in our potential and considered quantum numbers of the gluonic field as well. Combining with our relativistic corrections, the result has been the directly testable implications for the hadronic physics we report.

In our earlier work [1], properties of conventional and hybrid charmonium mesons were studied for radial ground states using an extended quark model. The investigation of radial excitations of mesons and hybrid mesons is of great interest in hadron physics. In Refs. [10,37], few radial excited states of conventional and hybrid charmonium mesons were predicted, although not with any potential model; Ref. [50] reports some orbital excitations of hybrids. In our present work, we calculate the masses, sizes, and radial wave functions of ground and radial excited state conventional $(\eta, J/\psi, h_c, \chi_o, \chi_1, \chi_2, \ldots)$ and hybrid charmonium states such as $0^{--}, 0^{+-}$, $1^{-+}, 2^{+-}, 3^{-+}, \ldots$ J^{PC} states. This present work is the extension of our previous work [1] along with relativistic corrections to it. In this present work, $E1$ and $M1$ radiative partial widths are also calculated for conventional meson to meson transitions and hybrid meson to hybrid meson transitions. As possible applications of our work, we would

TABLE I. Masses of ground and radially excited state charmonium mesons. Our calculated masses are rounded to 0.0001 GeV.

						Our calculated mass			
						Relativistic	NR	Theoretical mass [65] with NR potential model	Experimental mass
n	Meson	L	S	J	J^{PC}	GeV	GeV	GeV	GeV
$1S$	$\eta_c(1^1S_0)$	0	0	0	0^{-+}	2.99195	2.9816	2.982	2.9810 ± 0.0011 [67]
	$J/\psi(1^3S_1)$	0	1	1	1^{--}	3.0943	3.0900	3.090	3.096916 ± 0.000011 [67]
$2S$	$\eta_c'(2^1S_0)$	0	0	0	0^{-+}	3.6253	3.6303	3.630	3.6389 ± 0.0013 [67]
	$J/\psi(2^3S_1)$	0	1	1	1^{--}	3.6676	3.6718	3.672	$3.6861^{+0.000012}_{-0.000014}$ [67]
$3S$	$\eta_c(3^1S_0)$	0	0	0	0^{-+}	4.0294	4.0432	4.043	…
	$J/\psi(3^3S_1)$	0	1	1	1^{--}	4.0594	4.0716	4.072	4.040 ± 10 [65]
$4S$	$\eta_c(4^1S_0)$	0	0	0	0^{-+}	4.0594	4.3837	4.384	…
	$J/\psi(4^3S_1)$	0	1	1	1^{--}	4.3562	4.4061	4.406	4.415 ± 6 [65]
$5S$	$\eta_c(5^1S_0)$	0	0	0	0^{-+}	4.6393	4.6850	…	…
	$J/\psi(5^3S_1)$	0	1	1	1^{--}	4.6607	4.7038	…	
$6S$	$\eta_c(6^1S_0)$	0	0	0	0^{-+}	4.8928	4.9604	…	…
	$J/\psi(6^3S_1)$	0	1	1	1^{--}	4.9121	4.9769	…	…
$1P$	$h_c(1^1P_1)$	1	0	1	1^{+-}	3.5442	3.5156	3.516	3.52541 ± 0.00016 [67]
	$\chi_0(1^3P_0)$	1	1	0	0^{++}	3.4722	3.4245	3.424	3.41475 ± 0.00031 [67]
	$\chi_1(1^3P_1)$	1	1	1	1^{++}	3.5431	3.5054	3.505	3.51066 ± 0.00007 [67]
	$\chi_2(1^3P_2)$	1	1	2	2^{++}	3.584	3.5490	3.556	3.55620 ± 0.00009 [67]
$2P$	$h_c(2^1P_1)$	1	0	1	1^{+-}	3.9507	3.9336	3.934	…
	$\chi_0(2^3P_0)$	1	1	0	0^{++}	3.8847	3.8523	3.852	…
	$\chi_1(2^3P_1)$	1	1	1	1^{++}	3.9506	3.9249	3.925	…
	$\chi_2(2^3P_2)$	1	1	2	2^{++}	3.9938	3.9648	3.972	3.9272 ± 0.0026 [67]
$3P$	$h_c(3^1P_1)$	1	0	1	1^{+-}	4.2830	4.2793	4.279	…
	$\chi_0(3^3P_0)$	1	1	0	0^{++}	4.2186	4.2017	4.202	…
	$\chi_1(3^3P_1)$	1	1	1	1^{++}	4.2825	4.2707	4.271	…
	$\chi_2(3^3P_2)$	1	1	2	2^{++}	4.3275	4.3093	4.317	…
$4P$	$h_c(4^1P_1)$	1	0	1	1^{+-}	4.5714	4.5851	…	…
	$\chi_0(4^3P_0)$	1	1	0	0^{++}	4.5076	4.5092	…	…
	$\chi_1(4^3P_1)$	1	1	1	1^{++}	4.5702	4.5762	…	…
	$\chi_2(4^3P_2)$	1	1	2	2^{++}	4.6169	4.6141	…	…
$5P$	$h_c(5^1P_1)$	1	0	1	1^{+-}	4.8298	4.8644	…	…
	$\chi_0(5^3P_0)$	1	1	0	0^{++}	4.7659	4.7894	…	…
	$\chi_1(5^3P_1)$	1	1	1	1^{++}	4.8278	4.8552	…	…
	$\chi_2(5^3P_2)$	1	1	2	2^{++}	4.8759	4.8926	…	…
$6P$	$h_c(6^1P_1)$	1	0	1	1^{+-}	5.0654	5.1244	…	…
	$\chi_0(6^3P_0)$	1	1	0	0^{++}	5.0014	5.0500	…	…
	$\chi_1(6^3P_1)$	1	1	1	1^{++}	5.0628	5.1148	…	…
	$\chi_2(6^3P_2)$	1	1	2	2^{++}	5.1121	5.1520	…	…
$1D$	$\eta_{c2}(1^1D_2)$	2	0	2	2^{-+}	3.8372	3.7994	3.799	…
	$\psi(1^3D_1)$	2	1	1	1^{--}	3.8302	3.7850	3.785	3.7699 ± 0.0025 [65]
	$\psi_2(1^3D_2)$	2	1	2	2^{--}	3.8411	3.8004	3.800	…
	$\psi_3(1^3D_3)$	2	1	3	3^{--}	3.8441	3.8053	3.806	…
$2D$	$\eta_{c2}(2^1D_2)$	2	0	2	2^{-+}	4.1825	4.1576	4.158	…
	$\psi(2^3D_1)$	2	1	1	1^{--}	4.1737	4.1415	4.142	4.159 ± 0.020 [65]
	$\psi_2(2^3D_2)$	2	1	2	2^{--}	4.1867	4.1582	4.158	…
	$\psi_3(2^3D_3)$	2	1	3	3^{--}	4.1952	4.1655	4.167	…

(Table continued)

TABLE I. (*Continued*)

						Our calculated mass			
						Relativistic	NR	Theoretical mass [65] with NR potential model	Experimental mass
n	Meson	L	S	J	J^{PC}	GeV	GeV	GeV	GeV
$3D$	$\eta_{c2}(3^1D_2)$	2	0	2	2^{-+}	4.4802	4.4718	···	···
	$\psi(3^3D_1)$	2	1	1	1^{--}	4.4704	4.4547	···	···
	$\psi_2(3^3D_2)$	2	1	2	2^{--}	4.4846	4.4721	···	···
	$\psi_3(3^3D_3)$	2	1	3	3^{--}	4.4971	4.4810	···	···
$4D$	$\eta_{c2}(4^1D_2)$	2	0	2	2^{-+}	4.7456	4.7574	···	···
	$\psi(4^3D_1)$	2	1	1	1^{--}	4.7351	4.7395	···	···
	$\psi_2(4^3D_2)$	2	1	2	2^{--}	4.7502	4.7575	···	···
	$\psi_3(4^3D_3)$	2	1	3	3^{--}	4.7656	4.7675	···	···
$5D$	$\eta_{c2}(5^1D_2)$	2	0	2	2^{-+}	4.9870	5.0223	···	···
	$\psi(5^3D_1)$	2	1	1	1^{--}	4.9760	5.0039	···	···
	$\psi_2(5^3D_2)$	2	1	2	2^{--}	4.9918	5.0224	···	···
	$\psi_3(5^3D_3)$	2	1	3	3^{--}	5.0097	5.0331	···	···
$1F$	$h_{c3}(1^1F_3)$	3	0	3	3^{+-}	4.0690	4.0256	4.026	···
	$\chi_2(1^3F_2)$	3	1	2	2^{++}	4.0781	4.0290	4.029	···
	$\chi_3(1^3F_3)$	3	1	3	3^{++}	4.0735	4.0287	4.029	···
	$\chi_4(1^3F_4)$	3	1	4	4^{++}	4.06098	4.0212	4.021	···
$2F$	$h_{c3}(2^1F_3)$	3	0	3	3^{+-}	4.3783	4.3500	4.350	···
	$\chi_2(2^3F_2)$	3	1	2	2^{++}	4.3843	4.3506	4.351	···
	$\chi_3(2^3F_3)$	3	1	3	3^{++}	4.3823	4.3523	4.352	···
	$\chi_4(2^3F_4)$	3	1	4	4^{++}	4.3733	4.3477	4.348	···
$3F$	$h_{c3}(3^1F_3)$	3	0	3	3^{+-}	4.6526	4.6429	···	···
	$\chi_2(3^3F_2)$	3	1	2	2^{++}	4.6565	4.6417	···	···
	$\chi_3(3^3F_3)$	3	1	3	3^{++}	4.6563	4.6449	···	···
	$\chi_4(3^3F_4)$	3	1	4	4^{++}	4.6499	4.6422	···	···
$4F$	$h_{c3}(4^1F_3)$	3	0	3	3^{+-}	4.9011	4.9137	···	···
	$\chi_2(4^3F_2)$	3	1	2	2^{++}	4.9036	4.9111	···	···
	$\chi_3(4^3F_3)$	3	1	3	3^{++}	4.9048	4.9154	···	···
	$\chi_4(4^3F_4)$	3	1	4	4^{++}	4.9002	4.9141	···	···
$1G$	$\eta_{c4}(1^1G_4)$	4	0	4	4^{-+}	4.2717	4.2247	4225	···
	$\psi_3(1^3G_3)$	4	1	3	3^{--}	4.2890	4.2365	4.237	···
	$\psi_4(1^3G_4)$	4	1	4	4^{--}	4.2763	4.2282	4.228	···
	$\psi_5(1^3G_5)$	4	1	5	5^{--}	4.2577	4.2142	4.214	···

like to point out that using the radii, form factors [57,58], energy shifts [59,60], and magnetic polarizabilities [59] can be calculated for conventional and hybrid charmonium mesons. The decay constants [61,62], decay rates [61,63], and differential cross sections [64] for quarkonium states can be calculated using the radial wave function at the origin we report.

The paper is organized as follows. In Sec. II, the potential model used for conventional mesons is written. Then, using this potential model, radial wave functions for the ground and radially excited state conventional charmonium mesons are found by numerically solving the Schrödinger equation followed by relativistic improvements. The expressions used to find masses, root mean square radii, and radial wave functions at the origin for conventional charmonium mesons are written in this section, along with those for finding the $M1$ and $E1$ radiative transition widths. In Sec. III, the potential model is written for hybrid mesons, and then we accordingly (i.e., for hybrids) redo all the numerical work, as done in Sec. II. Results for the masses, root mean square radii, and squares of radial wave functions at the origin for the radial and orbital ground and excited states of conventional and hybrid charmonium mesons are reported in Sec. IV. Radiative partial widths are

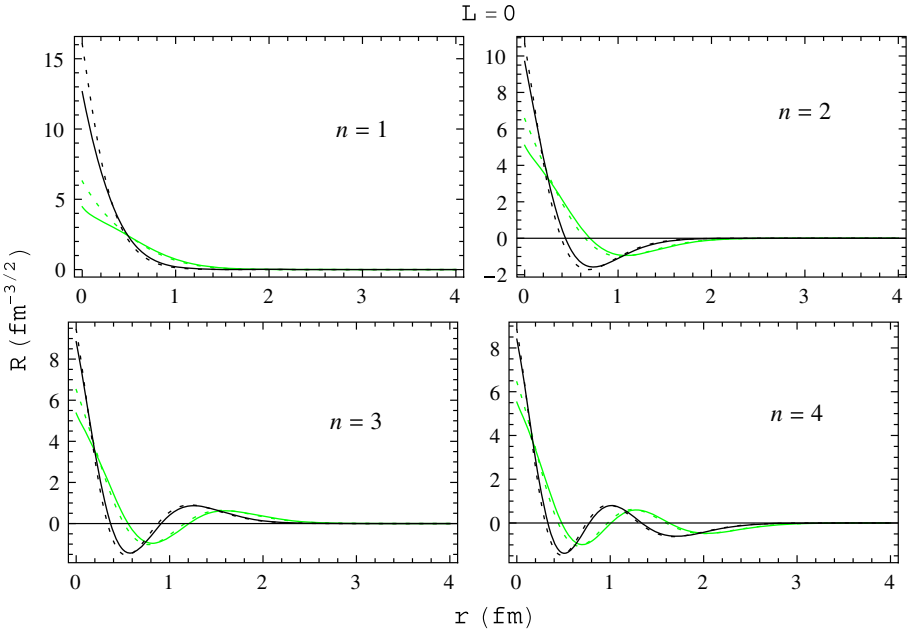

FIG. 1 (color online). Radial wave functions for radially ground and excited states of η_c and J/ψ mesons. The black line curves represent mesons, and the green line curves represent hybrid mesons. Solid line curves are for J/ψ, and dotted curves are for η_c.

also reported in this section. Based on these results, we also include some results related to experimentally measurable quantities. In Sec. IV, XYZ particles are related with different states of charmonium mesons based on similar mass and J^{PC} values where available.

II. CONVENTIONAL CHARMONIUM MESONS

For the conventional mesons, we use the following quark-antiquark effective potential [65]:

$$V_{q\bar{q}}(r) = \frac{-4\alpha_s}{3r} + br + \frac{32\pi\alpha_s}{9m_c^2}\left(\frac{\sigma}{\sqrt{\pi}}\right)^3 e^{-\sigma^2 r^2}\vec{S}_c\cdot\vec{S}_{\bar{c}} + \frac{1}{m_c^2}\left[\left(\frac{2\alpha_s}{r^3}-\frac{b}{2r}\right)\vec{L}\cdot\vec{S}+\frac{4\alpha_s}{r^3}T\right], \quad (1)$$

where the first term is due to one gluon exchange with the quark-gluon coupling constant α_s, the second is the linear confining potential with string tension b, the third term is the Gaussian-smeared hyperfine interaction, and the last term is for the spin-orbit potential with

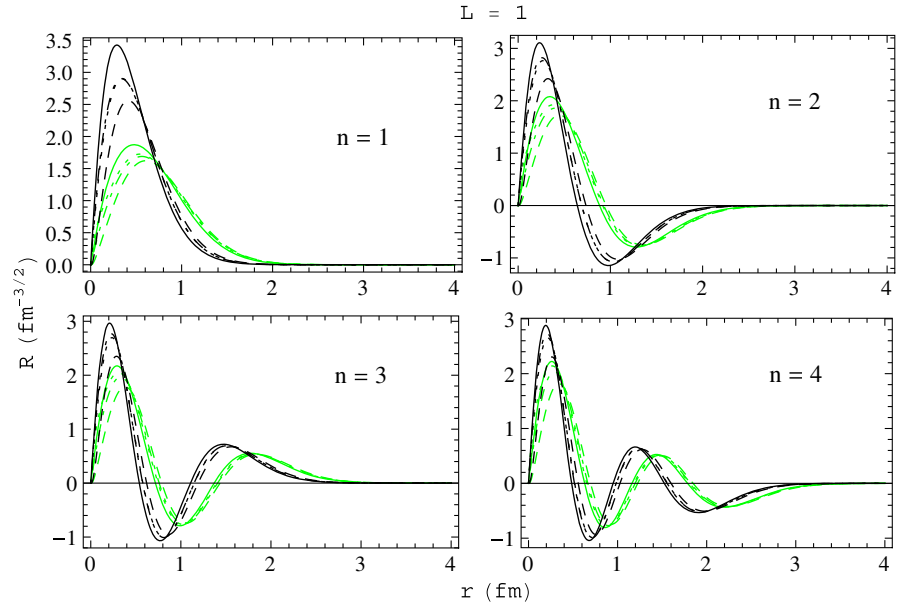

FIG. 2 (color online). Radial wave functions for radially ground and excited states of $\chi_{c_0}, \chi_{c_1}, \chi_{c_2}$, and h_c. Solid line curves are for χ_{c_0}, dotted line curves for χ_{c_1}, dashed line curves for χ_{c_2}, and dot-dashed line curves for h_c. Black line curves represent mesons, and green line curves represent hybrid mesons.

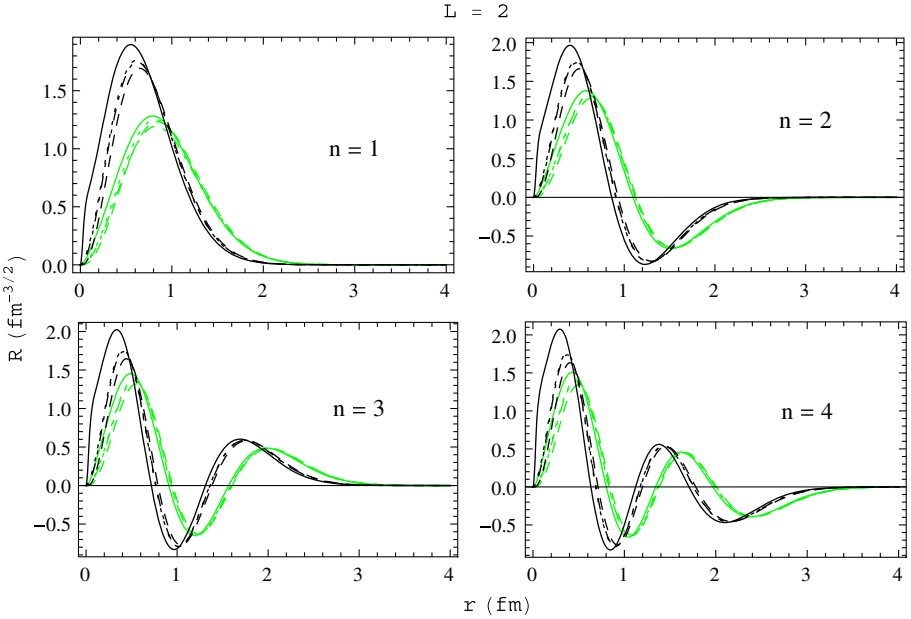

FIG. 3 (color online). Radial wave functions for radially ground and excited states of ψ_1, ψ_2, ψ_3, and η_{c_2}. Solid line curves are for ψ_1, dotted line curves for ψ_2, dashed line curves for ψ_3, and dot-dashed line curves for η_{c_2}. Black line curves represent mesons, and green line curves represent hybrid mesons.

$$\vec{L}\cdot\vec{S} = [J(J+1) - L(L+1) - S(S+1)]/2 \qquad (2)$$

and

$$\langle {}^3L_J|T|{}^3L_J\rangle = \begin{cases} -\frac{1}{6(2L+3)}, & J = L+1 \\ +\frac{1}{6}, & J = L \\ -\frac{L+1}{6(2L-1)}, & J = L-1. \end{cases} \qquad (3)$$

Here, L and S are quantum numbers of the relative orbital angular momentum of the quark-antiquark and the total spin angular momentum of the meson, respectively. The spin-orbit potential and the tensor term are both 0 [65] for the angular momentum $L = 0$. The parameters used in this potential for the charm quark and antiquark are taken to be $\alpha_s = 0.5461$, $b = 0.1425$ GeV^2, $\sigma = 1.0946$ GeV, and $m_c = 1.4796$ GeV, as in Refs. [1,65]. These values are obtained from the fit of the masses of 11 experimentally known $c\bar{c}$ states mentioned in the last column of Table I.

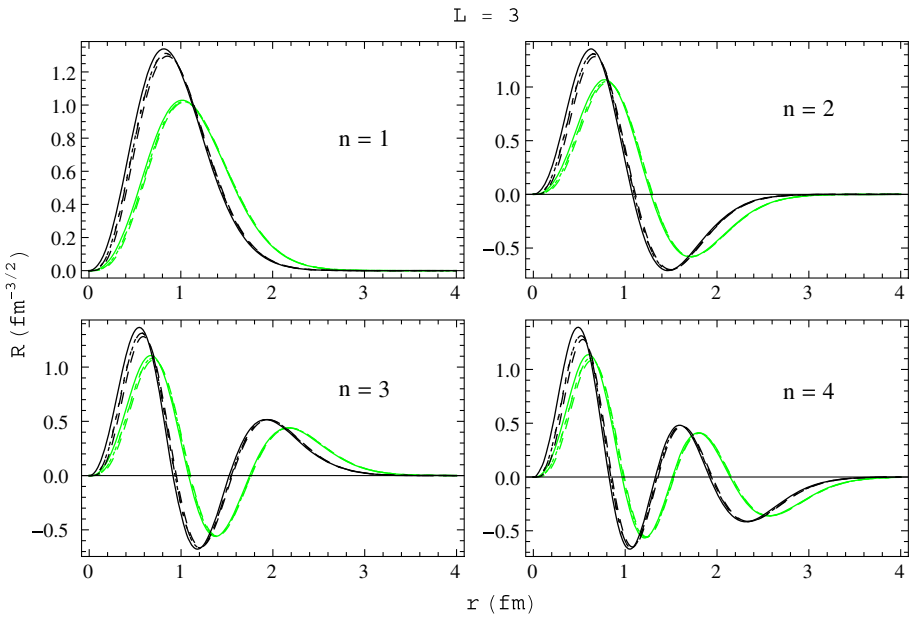

FIG. 4 (color online). Radial wave functions for radially ground and excited states of χ_2, χ_3, χ_4, and h_{c_3}. Solid line curves are for χ_2, dotted line curves for χ_3, dashed line curves for χ_4, and dot-dashed line curves for h_{c_3}. Black line curves represent mesons, and green line curves represent hybrid mesons.

TABLE II. Our calculated masses of $c\bar{c}$ hybrid charmonium mesons.

							Our calculated mass	
					J^{PC}		Relativistic	NR
n	Meson	L	S	J	$\varepsilon = 1$	$\varepsilon = -1$	GeV	GeV
$1S$	$\eta_c^h(1^1S_0)$	0	0	0	0^{++}	0^{--}	4.1477	4.0802
	$J/\psi^h(1^3S_1)$	0	1	1	1^{+-}	1^{-+}	4.1707	4.1063
$2S$	$\eta_c^h(2^1S_0)$	0	0	0	0^{++}	0^{--}	4.4594	4.3820
	$J/\psi^h(2^3S_1)$	0	1	1	1^{+-}	1^{-+}	4.4837	4.4084
$3S$	$\eta_c^h(3^1S_0)$	0	0	0	0^{++}	0^{--}	4.73897	4.6616
	$J/\psi^h(3^3S_1)$	0	1	1	1^{+-}	1^{-+}	4.7614	4.6855
$4S$	$\eta_c^h(4^1S_0)$	0	0	0	0^{++}	0^{--}	4.9928	4.9223
	$J/\psi^h(4^3S_1)$	0	1	1	1^{+-}	1^{-+}	5.0132	4.9438
$5S$	$\eta_c^h(5^1S_0)$	0	0	0	0^{++}	0^{--}	5.2261	5.1683
	$J/\psi^h(5^3S_1)$	0	1	1	1^{+-}	1^{-+}	5.2448	5.1876
$6S$	$\eta_c^h(6^1S_0)$	0	0	0	0^{++}	0^{--}	5.4429	5.4021
	$J/\psi^h(6^3S_1)$	0	1	1	1^{+-}	1^{-+}	5.4602	5.4197
$1P$	$h_c^h(1^1P_1)$	1	0	1	1^{--}	1^{++}	4.3372	4.2678
	$\chi_0^h(1^3P_0)$	1	1	0	0^{-+}	0^{+-}	4.3203	4.2464
	$\chi_1^h(1^3P_1)$	1	1	1	1^{-+}	1^{+-}	4.3398	4.2678
	$\chi_2^h(1^3P_2)$	1	1	2	2^{-+}	2^{+-}	4.3430	4.2739
$2P$	$h_c^h(2^1P_1)$	1	0	1	1^{--}	1^{++}	4.6309	4.5552
	$\chi_0^h(2^3P_0)$	1	1	0	0^{-+}	0^{+-}	4.6070	4.5264
	$\chi_1^h(2^3P_1)$	1	1	1	1^{-+}	1^{+-}	4.6327	4.5538
	$\chi_2^h(2^3P_2)$	1	1	2	2^{-+}	2^{+-}	4.6424	4.5653
$3P$	$h_c^h(3^1P_1)$	1	0	1	1^{--}	1^{++}	4.8943	4.8210
	$\chi_0^h(3^3P_0)$	1	1	0	0^{-+}	0^{+-}	4.8659	4.7875
	$\chi_1^h(3^3P_1)$	1	1	1	1^{-+}	1^{+-}	4.8955	4.8188
	$\chi_2^h(3^3P_2)$	1	1	2	2^{-+}	2^{+-}	4.9098	4.8337
$4P$	$h_c^h(4^1P_1)$	1	0	1	1^{--}	1^{++}	5.1349	5.0707
	$\chi_0^h(4^3P_0)$	1	1	0	0^{-+}	0^{+-}	5.1034	5.0338
	$\chi_1^h(4^3P_1)$	1	1	1	1^{-+}	1^{+-}	5.1358	5.0678
	$\chi_2^h(4^3P_2)$	1	1	2	2^{-+}	2^{+-}	5.15355	5.0852
$5P$	$h_c^h(5^1P_1)$	1	0	1	1^{1--}	1^{++}	5.3577	5.3076
	$\chi_0^h(5^3P_0)$	1	1	0	0^{-+}	0^{+-}	5.3236	5.2682
	$\chi_1^h(5^3P_1)$	1	1	1	1^{-+}	1^{+-}	5.3582	5.3042
	$\chi_2^h(5^3P_2)$	1	1	2	2^{-+}	2^{+-}	5.3786	5.3233
$6P$	$h_c^h(6^1P_1)$	1	0	1	1^{--}	1^{++}	5.5656	5.5340
	$\chi_0^h(6^3P_0)$	1	1	0	0^{-+}	0^{+-}	5.5294	5.4925
	$\chi_1^h(6^3P_1)$	1	1	1	1^{-+}	1^{+-}	5.5657	5.5301
	$\chi_2^h(6^3P_2)$	1	1	2	2^{-+}	2^{+-}	5.5885	5.5507
$1D$	$\eta_{c2}(1^1D_2)$	2	0	2	2^{++}	2^{--}	4.4985	4.4222
	$\psi^h(1^3D_1)$	2	1	1	1^{+-}	1^{-+}	4.4320	4.4232
	$\psi_2^h(1^3D_2)$	2	1	2	2^{+-}	2^{-+}	4.5029	4.4251
	$\psi_3^h(1^3D_3)$	2	1	3	3^{+-}	3^{-+}	4.4944	4.4197
$2D$	$\eta_{c2}^h(2^1D_2)$	2	0	2	2^{++}	2^{--}	4.7761	4.6982
	$\psi^h(2^3D_1)$	2	1	1	1^{+-}	1^{-+}	4.6892	4.6955
	$\psi_2^h(2^3D_2)$	2	1	2	2^{+-}	2^{-+}	4.7797	4.7002
	$\psi_3^h(2^3D_3)$	2	1	3	3^{+-}	3^{-+}	4.7757	4.6981

(Table continued)

TABLE II. (*Continued*)

					J^{PC}		Our calculated mass	
							Relativistic	NR
n	Meson	L	S	J	$\varepsilon = 1$	$\varepsilon = -1$	GeV	GeV
$3D$	$\eta_{c2}^h(3^1D_2)$	2	0	2	2^{++}	2^{--}	5.0274	4.9554
	$\psi^h(3^3D_1)$	2	1	1	1^{+-}	1^{-+}	4.96605	4.9402
	$\psi_2^h(3^3D_2)$	2	1	2	2^{+-}	2^{-+}	5.0308	4.9569
	$\psi_3^h(3^3D_3)$	2	1	3	3^{+-}	3^{-+}	5.0301	4.9572
$4D$	$\eta_{c2}^h(4^1D_2)$	2	0	2	2^{++}	2^{--}	5.2585	5.1983
	$\psi^h(4^3D_1)$	2	1	1	1^{+-}	1^{-+}	5.2034	5.1912
	$\psi_2^h(4^3D_2)$	2	1	2	2^{+-}	2^{-+}	5.2618	5.1994
	$\psi_3^h(4^3D_3)$	2	1	3	3^{+-}	3^{-+}	5.2638	5.2014
$5D$	$\eta_{c2}^h(1^1D_2)$	2	0	2	2^{++}	2^{--}	5.4733	5.4295
	$\psi^h(5^3D_1)$	2	1	1	1^{+-}	1^{-+}	5.4287	5.4210
	$\psi_2^h(5^3D_2)$	2	1	2	2^{+-}	2^{-+}	5.4765	5.4304
	$\psi_3^h(5^3D_3)$	2	1	3	3^{+-}	3^{-+}	5.4809	5.4338
$1F$	$h_{c3}^h(1^1F_3)$	3	0	3	3^{--}	3^{++}	4.6517	4.5700
	$\chi_2^h(1^3F_2)$	3	1	2	2^{-+}	2^{+-}	4.6649	4.5790
	$\chi_3^h(1^3F_3)$	3	1	3	3^{-+}	3^{+-}	4.6562	4.5735
	$\chi_4^h(1^3F_4)$	3	1	4	4^{-+}	4^{+-}	4.6408	4.5623
$2F$	$h_{c3}^h(2^1F_3)$	3	0	3	3^{--}	3^{++}	4.91395	4.8350
	$\chi_2^h(2^3F_2)$	3	1	2	2^{-+}	2^{+-}	4.9241	4.8412
	$\chi_3^h(2^3F_3)$	3	1	3	3^{-+}	3^{+-}	4.9179	4.8379
	$\chi_4^h(2^3F_4)$	3	1	4	4^{-+}	4^{+-}	4.9056	4.8293
$3F$	$h_{c3}^h(3^1F_3)$	3	0	3	3^{--}	3^{++}	5.1538	5.084
	$\chi_2^h(3^3F_2)$	3	1	2	2^{-+}	2^{+-}	5.1617	5.0881
	$\chi_3^h(3^3F_3)$	3	1	3	3^{-+}	3^{+-}	5.1574	5.0864
	$\chi_4^h(3^3F_4)$	3	1	4	4^{-+}	4^{+-}	5.1474	5.0798
$4F$	$h_{c3}^h(4^1F_3)$	3	0	3	3^{--}	3^{++}	5.3759	5.3203
	$\chi_2^h(4^3F_2)$	3	1	2	2^{-+}	2^{+-}	5.3820	5.3228
	$\chi_3^h(4^3F_3)$	3	1	3	3^{-+}	3^{+-}	5.3791	5.3224
	$\chi_4^h(4^3F_4)$	3	1	4	4^{-+}	4^{+-}	5.3710	5.3173

In the third term $\vec{S}_c \cdot \vec{S}_{\bar{c}} = \frac{S(S+1)}{2} - \frac{3}{4}$, μ is the reduced mass of the quark and antiquark, and m_c is the constituent mass of the charm quark. The values of quantum numbers L and S which we choose for our study are reported in Table I. In the quark model, the characteristics of a conventional meson can be described by the wave function of the bound state of the quark and antiquark. This wave function $U(r) = rR(r)$ can be found by solving the radial Schrödinger equation given as

$$U''(r) + 2\mu\left(E - V(r) - \frac{L(L+1)}{2\mu r^2}\right)U(r) = 0. \qquad (4)$$

$R(r)$ is the radial wave function, and r is the interquark distance. Here, E is the sum of the kinetic and potential energy of the quark-antiquark system. In this nonrelativistic approximation, which we improve on below, the mass of a $c\bar{c}$ state is obtained after the addition of constituent quark masses in the energy E. We found the numerical solution of the Schrödinger equation using the shooting method. Earlier [1], we used this method to find the numerical solutions for the radial ground state (i.e., for $n = 1$). Now, we extend this work of Ref. [1] by finding the normalized solutions for the radial ground and excited states (i.e., for $n = 1, 2, 3, 4, \ldots$). It is noted that in the limit $r \to 0$, the potential $V(r) \sim \frac{2\alpha_s}{r^3}(\vec{L} \cdot \vec{S} + 2T)$. It turns out that $\vec{L} \cdot \vec{S} + 2T$ is negative for $J = L$ and $J = L - 1$. As a result, the potential becomes strongly attractive at a short distance and the resultant wave function becomes unstable in this limit. To circumvent this problem, we calculated the meson masses by initially solving the Schrödinger equation without spin-orbit coupling. The effect of spin-orbit interaction was subsequently included through leading-order perturbative correction to the meson mass. As a check on our

TABLE III. Our assignments based on the equivalence of predicted and experimental values of masses and J^{PC}.

Meson	J^{PC}	Experimental mass GeV	Assignments
$\chi_{c_2}(2P)$	2^{++}	3.9272 ± 2.6 [67]	$\chi_2(2^3P_2)$
$h_c(1^1P_1)$	1^{+-}	3.52538 ± 0.11 [67]	$h_c(1^1P_1)$
$X(3872)$	1^{++}	3.87168 ± 0.17 [67]	$\chi_1(2^3P_1)$
	$?^{?+}$		$\chi_0(2^3P_0)$, $\chi_1(2^3P_1)$, $\chi_2(2^3P_2)$, $\eta_{c2}(1^1D_2)$
$X(4260)$	1^{--}	4.250 ± 9 [67]	$\psi(2^3D_1)$, $\psi(3^3S_1)$, $h_c^h(1^1P_1)$
$X(3915)$	0^{++}	$3.918.4 \pm 1.9$ [67]	$\chi_0(2^3P_0)$, $\eta_c^h(1^1S_0)$
	$?^{?+}$		$\eta_c(3^1S_0)$, $\chi_0(2^3P_0)$, $\chi_1(2^3P_1)$, $\chi_2(2^3P_2)$,$\eta_{c2}(1^1D_2)$
$X(4360)$	1^{--}	4.361 ± 13 [67]	$\psi(3^3D_1)$, $J/\psi(4^3S_1)$, $h_c^h(1^1P_1)$
$Y(4360)$			
$X(4660)$	1^{--}	4.664 ± 12 [67]	$J/\psi(5^3S_1)$, $\psi(3^3D_1)$, $\psi(4^3D_1)$
			$h_c^h(2^1P_1)$
$X(3940)$	1^{--}	3.942^{+9}_{-8} [71]	$J/\psi(3^3S_1)$, $\psi(1^3D_1)$
$X(4350)$	1^{--}	$4.3506\pm^{+4.6}_{-5.1}$ [5,71]	$J/\psi(4^3S_1)$, $\psi(2^3D_1)$, $\psi(3^3D_1)$, $h_c^h(1^1P_1)$
$X(4008)$	1^{--}	4.008^{+121}_{-49} [71]	$\psi(3^3S_1)$,$\psi(2^3D_1)$
$X(3940)$	1^{++}	…	$\chi_1(2^3P_0)$
$X(4630)$	1^{--}	4.634^{+9}_{-11} [71]	$J/\psi(5^3S_1)$, $\psi(3^3D_1)$, $\psi(4^3D_1)$, $h_c^h(2^1P_1)$
$Y(4630)$			
$Y(4350)$	0^{++}	$4.3506^{+4.6}_{-5.1}$ [71]	$\chi_0(3^3P_0)$, $\eta_c^h(2^1S_0)$
	2^{++}	$4.3506^{+4.6}_{-5.1}$ [71]	$\chi_2(3^3P_2)$, $\chi_2(2^3F_2)$, $\eta_{c2}^h(1^1D_2)$
$\eta_{c2}(1D)$	2^{-+}	…	$\eta_{c2}(1^1D_2)$

calculation, we confirmed that our results for the charmonium meson masses using the nonrelativistic (NR) potential for ground and radially excited states agree with Table I of Ref. [65]. The black curves in Figs. 1–4 show the radial wave functions $R(r)$ of charmonium mesons for different values of n, L, and S. Four panels in each figure correspond to four values of $n = 1$, 2, 3, and 4, respectively, and four black curves in each panel correspond to four possible values of J corresponding to each value of L, which are taken as 0, 1, 2, and 3 in Figs. 1,2,3, and 4, respectively. The exception of two black curves in each panel of Fig. 1 arises because for $L = 0$, the quantum number J can have only two possible values. We noted that for $L > 0$, $R(0) = 0$ and $R(r)$ decrease exponentially at large interquark distances. The number of nodes in a radial wave function is equal to $n - 1$. It is also noted that peaks come closer to

TABLE IV. Masses (in GeV) of hybrid charmonium mesons calculated by others with different models along with our calculated results. Our results are reported for the least J^{PC} states.

	Our results				Lattice QCD		
					Ground state		
J^{PC} state	Ground state	First radial excited state	Flux-tube model [20]	Constituent glue model [16]	[72]	[32]	First radial excited state [32]
0^{--}	4.0983	4.4012	…	4.35	…	…	
0^{+-}	4.26599	4.5475	4.19	…	~4.35	~4.382	…
0^{-+}	4.26599	4.5475	4.19	4.38	~4.120	…	…
1^{-+}	4.1242	4.4284	4.19	4.48	~4.300	~4.213	
1^{++}	4.2859	4.5748	4.19	…	…	…	…
1^{+-}	4.1242	4.4284	4.19	…	…	…	…
1^{--}	4.2859	4.5748	4.19	4.27	4.189(54)	…	…
2^{-+}	4.2917	4.5849	4.19	…	~4.300	…	…
2^{+-}	4.2917	4.5849	4.19	…	4.4	~4.391	~4.505
3^{-+}	4.4386	4.7178	…	…	4.7		

TABLE V. Root mean square radii and square of the radial wave function at the origin for ground and radially excited state conventional charmonium mesons.

n	Meson	L	S	J	J^{PC}	Our calculated $\sqrt{\langle r^2\rangle}$ fm	Theoretical $\sqrt{\langle r^2\rangle}$ with potential model [73] fm	Our calculated $\lvert R(0)\rvert^2$ GeV^3
$1S$	$\eta_c(1^1S_0)$	0	0	0	0^{-+}	0.3655	0.388	1.2294
	$J/\psi(1^3S_1)$	0	1	1	1^{--}	0.4143	0.404	1.97675
$2S$	$\eta_c(2^1S_0)$	0	0	0	0^{-+}	0.8328	⋯	0.8717
	$J/\psi(2^3S_1)$	0	1	1	1^{--}	0.8627	⋯	0.7225
$3S$	$\eta_c(3^1S_0)$	0	0	0	0^{-+}	1.2072	⋯	0.683
	$J/\psi(3^3S_1)$	0	1	1	1^{--}	1.2287	⋯	0.6006
$4S$	$\eta_c(4^1S_0)$	0	0	0	0^{-+}	1.5306	⋯	0.5994
	$J/\psi(4^3S_1)$	0	1	1	1^{--}	1.5478	⋯	0.5417
$5S$	$\eta_c(5^1S_0)$	0	0	0	0^{-+}	1.8225	⋯	0.5503
	$J/\psi(5^3S_1)$	0	1	1	1^{--}	1.8370	⋯	0.50538
$6S$	$\eta_c(6^1S_0)$	0	0	0	0^{-+}	2.0922	⋯	0.5172
	$J/\psi(6^3S_1)$	0	1	1	1^{--}	2.1048	⋯	0.4801
$1P$	$h_c(1^1P_1)$	1	0	1	1^{+-}	0.6738	0.602	≈0
	$\chi_0(1^3P_0)$	1	1	0	0^{++}	0.621	0.606	≈0
	$\chi_1(1^3P_1)$	1	1	1	1^{++}	0.6475	⋯	≈0
	$\chi_2(1^3P_2)$	1	1	2	2^{++}	0.7173	⋯	≈0
$2P$	$h_c(2^1P_1)$	1	0	1	1^{+-}	1.0697	⋯	≈0
	$\chi_0(2^3P_0)$	1	1	0	0^{++}	1.0374	⋯	≈0
	$\chi_1(2^3P_1)$	1	1	1	1^{++}	1.0437	⋯	≈0
	$\chi_2(2^3P_2)$	1	1	2	2^{++}	1.1107	⋯	≈0
$3P$	$h_c(3^1P_1)$	1	0	1	1^{+-}	1.4052	⋯	≈0
	$\chi_0(3^3P_0)$	1	1	0	0^{++}	1.3814	⋯	≈0
	$\chi_1(3^3P_1)$	1	1	1	1^{++}	1.3786	⋯	≈0
	$\chi_2(3^3P_2)$	1	1	2	2^{++}	1.4444	⋯	≈0
$4P$	$h_c(4^1P_1)$	1	0	1	1^{+-}	1.7054	⋯	≈0
	$\chi_0(4^3P_0)$	1	1	0	0^{++}	1.6863	⋯	≈0
	$\chi_1(4^3P_1)$	1	1	1	1^{++}	1.6782	⋯	≈0
	$\chi_2(4^3P_2)$	1	1	2	2^{++}	1.7433	⋯	≈0
$5P$	$h_c(5^1P_1)$	1	0	1	1^{+-}	1.9815	⋯	≈0
	$\chi_0(5^3P_0)$	1	1	0	0^{++}	1.9654	⋯	≈0
	$\chi_1(5^3P_1)$	1	1	1	1^{++}	1.9537	⋯	≈0
	$\chi_2(5^3P_2)$	1	1	2	2^{++}	2.0183	⋯	≈0
$6P$	$h_c(6^1P_1)$	1	0	1	1^{+-}	2.2397	⋯	≈0
	$\chi_0(6^3P_0)$	1	1	0	0^{++}	2.2257	⋯	≈0
	$\chi_1(6^3P_1)$	1	1	1	1^{++}	2.2115	⋯	≈0
	$\chi_2(6^3P_2)$	1	1	2	2^{++}	2.2755	⋯	≈0
$1D$	$\eta_{c2}(1^1D_2)$	2	0	2	2^{-+}	0.8984	⋯	≈0
	$\psi(1^3D_1)$	2	1	1	1^{--}	0.8432	⋯	≈0
	$\psi_2(1^3D_2)$	2	1	2	2^{--}	0.8938	⋯	≈0
	$\psi_3(1^3D_3)$	2	1	3	3^{--}	0.9179	⋯	≈0

n	Meson	L	S	J	J^{PC}	Our calculated $\sqrt{\langle r^2\rangle}$ fm	$\lvert R(0)\rvert^2$ GeV^3
$2D$	$\eta_{c2}(2^1D_2)$	2	0	2	2^{-+}	1.2595	≈0
	$\psi(2^3D_1)$	2	1	1	1^{--}	1.1914	≈0

(Table continued)

TABLE V. (*Continued*)

n	Meson	L	S	J	J^{PC}	Our calculated $\sqrt{\langle r^2\rangle}$ fm	$\lvert R(0)\rvert^2$ GeV^3
	$\psi_2(2^3D_2)$	2	1	2	2^{--}	1.2558	≈0
	$\psi_3(2^3D_3)$	2	1	3	3^{--}	1.2788	≈0
$3D$	$\eta_{c2}(3^1D_2)$	2	0	2	2^{-+}	1.5740	≈0
	$\psi(3^3D_1)$	2	1	1	1^{--}	1.4897	≈0
	$\psi_2(3^3D_2)$	2	1	2	2^{--}	1.5708	≈0
	$\psi_3(3^3D_3)$	2	1	3	3^{--}	1.5934	≈0
$4D$	$\eta_{c2}(4^1D_2)$	2	0	2	2^{-+}	1.8596	≈0
	$\psi(4^3D_1)$	2	1	1	1^{--}	1.7574	≈0
	$\psi_2(4^3D_2)$	2	1	2	2^{--}	1.8566	≈0
	$\psi_3(4^3D_3)$	2	1	3	3^{--}	1.8793	≈0
$5D$	$\eta_{c2}(5^1D_2)$	2	0	2	2^{-+}	2.1248	≈0
	$\psi(5^3D_1)$	2	1	1	1^{--}	2.0049	≈0
	$\psi_2(5^3D_2)$	2	1	2	2^{--}	2.1219	≈0
	$\psi_3(5^3D_3)$	2	1	3	3^{--}	2.1446	≈0
$1F$	$h_{c3}(1^1F_3)$	3	0	3	3^{+-}	1.0878	≈0
	$\chi_2(1^3F_2)$	3	1	2	2^{++}	1.0690	≈0
	$\chi_3(1^3F_3)$	3	1	3	3^{++}	1.0863	≈0
	$\chi_4(1^3F_4)$	3	1	4	4^{++}	1.0982	≈0
$2F$	$h_{c3}(2^1F_3)$	3	0	3	3^{+-}	1.4253	≈0
	$\chi_2(2^3F_2)$	3	1	2	2^{++}	1.4066	≈0
	$\chi_3(2^3F_3)$	3	1	3	3^{++}	1.4239	≈0
	$\chi_4(2^3F_4)$	3	1	4	4^{++}	1.4356	≈0
$3F$	$h_{c3}(3^1F_3)$	3	0	3	3^{+-}	1.7250	≈0
	$\chi_2(3^3F_2)$	3	1	2	2^{++}	1.7062	≈0
	$\chi_3(3^3F_3)$	3	1	3	3^{++}	1.7238	≈0
	$\chi_4(3^3F_4)$	3	1	4	4^{++}	1.7355	≈0
$4F$	$h_{c3}(4^1F_3)$	3	0	3	3^{+-}	2.0000	≈0
	$\chi_2(4^3F_2)$	3	1	2	2^{++}	1.9810	≈0
	$\chi_3(4^3F_3)$	3	1	3	3^{++}	1.9989	≈0
	$\chi_4(4^3F_4)$	3	1	4	4^{++}	2.0108	≈0
$1G$	$\eta_{c4}(1^1G_4)$	4	0	4	4^{-+}	1.2589	≈0
	$\psi_3(1^3G_3)$	4	1	3	3^{--}	1.2501	≈0
	$\psi_4(1^3G_4)$	4	1	4	4^{--}	1.2588	≈0
	$\psi_5(1^3G_5)$	4	1	5	5^{--}	1.2642	≈0

the origin as we go to higher radially excited states. And, by increasing L, the wave function's peak goes away from the origin. But, the wave functions are essentially insensitive to the S values. One possible reason is that for our heavy quarks, the $1/m_c^2$ factor [appearing in Eq. (1)] of the hyperfine term becomes very small. The normalized wave functions are then used to calculate root mean square radii and radial wave functions at the origin using the following relations:

$$\sqrt{\langle r^2\rangle} = \sqrt{\int U^\star r^2 U dr}, \tag{5}$$

$$R(0) = U'(0) \quad \text{for } l = 0. \tag{6}$$

The radial wave function at the origin is used in many applications of high energy physics, as mentioned in Sec. I. As discussed above, $\frac{1}{r^3}$ terms make the wave function unstable at a small distance whenever $J = L$ or $J = L - 1$. In the case of mass calculation, the problem is overcome by treating the spin-orbit coupling through perturbation theory. However, calculating the perturbative correction to the wave function is difficult, as, in this case, the contributions come from all possible mass eigenstates. Therefore, in this case, we applied the smearing of position

TABLE VI. Our calculated root mean square radii and $|R(0)|^2$ of $c\bar{c}$ hybrid mesons.

					J^{PC}		Our calculated $\sqrt{\langle r^2 \rangle}$	Our calculated $\lvert R(0)\rvert^2$
n	Meson	L	S	J	$\varepsilon = 1$	$\varepsilon = -1$	fm	Gev^3
$1S$	$\eta_c^h(1^1S_0)$	0	0	0	0^{++}	0^{--}	0.6429	0.30458
	$J/\psi^h(1^3S_1)$	0	1	1	1^{+-}	1^{-+}	0.6949	0.1533
$2S$	$\eta_c'^h(2^1S_0)$	0	0	0	0^{++}	0^{--}	1.0837	0.3306
	$J/\psi^h(2^3S_1)$	0	1	1	1^{+-}	1^{-+}	1.1187	0.1995
$3S$	$\eta_c^h(3^1S_0)$	0	0	0	0^{++}	0^{--}	1.4345	0.3259
	$J/\psi^h(3^3S_1)$	0	1	1	1^{+-}	1^{-+}	1.4608	0.2214
$4S$	$\eta_c^h(4^1S_0)$	0	0	0	0^{++}	0^{--}	1.7413	0.3189
	$J/\psi^h(4^3S_1)$	0	1	1	1^{+-}	1^{-+}	1.7624	0.2342
$5S$	$\eta_c^h(5^1S_0)$	0	0	0	0^{++}	0^{--}	2.0203	0.3128
	$J/\psi^h(5^3S_1)$	0	1	1	1^{+-}	1^{-+}	2.0379	0.2425
$6S$	$\eta_c^h(6^1S_0)$	0	0	0	0^{++}	0^{--}	2.2796	0.3078
	$J/\psi^h(6^3S_1)$	0	1	1	1^{+-}	1^{-+}	2.2948	0.2482
$1P$	$h_c^h(1^1P_1)$	1	0	1	1^{--}	1^{++}	0.9224	≈ 0
	$\chi_0^h(1^3P_0)$	1	1	0	0^{-+}	0^{+-}	0.8826	≈ 0
	$\chi_1^h(1^3P_1)$	1	1	1	1^{-+}	1^{+-}	0.9106	≈ 0
	$\chi_2^h(1^3P_2)$	1	1	2	2^{-+}	2^{+-}	0.9451	≈ 0
$2P$	$h_c^h(2^1P_1)$	1	0	1	1^{--}	1^{++}	1.2954	≈ 0
	$\chi_0^h(2^3P_0)$	1	1	0	0^{-+}	0^{+-}	1.2738	≈ 0
	$\chi_1^h(2^3P_1)$	1	1	1	1^{-+}	1^{+-}	1.2826	≈ 0
	$\chi_2^h(2^3P_2)$	1	1	2	2^{-+}	2^{-+}	1.3208	≈ 0
$3P$	$h_c^h(3^1P_1)$	1	0	1	1^{--}	1^{++}	1.6139	≈ 0
	$\chi_0^h(3^3P_0)$	1	1	0	0^{-+}	0^{+-}	1.6036	≈ 0
	$\chi_1^h(3^3P_1)$	1	1	1	1^{-+}	1^{+-}	1.5999	≈ 0
	$\chi_2^h(3^3P_2)$	1	1	2	2^{-+}	2^{-+}	1.6408	≈ 0
$4P$	$h_c^h(4^1P_1)$	1	0	1	1^{--}	1^{++}	1.9009	≈ 0
	$\chi_0^h(4^3P_0)$	1	1	0	0^{-+}	0^{+-}	1.8982	≈ 0
	$\chi_1^h(4^3P_1)$	1	1	1	1^{-+}	1^{+-}	1.8857	≈ 0
	$\chi_2^h(4^3P_2)$	1	1	2	2^{-+}	2^{-+}	1.9287	≈ 0
$5P$	$h_c^h(5^1P_1)$	1	0	1	1^{1--}	1^{++}	2.1663	≈ 0
	$\chi_0^h(5^3P_0)$	1	1	0	0^{-+}	0^{+-}	2.1690	≈ 0
	$\chi_1^h(5^3P_1)$	1	1	1	1^{-+}	1^{+-}	2.1498	≈ 0
	$\chi_2^h(5^3P_2)$	1	1	2	2^{-+}	2^{-+}	2.1945	≈ 0
$6P$	$h_c^h(6^1P_1)$	1	0	1	1^{--}	1^{++}	2.4155	≈ 0
	$\chi_0^h(6^3P_0)$	1	1	0	0^{-+}	0^{+-}	2.4223	≈ 0
	$\chi_1^h(6^3P_1)$	1	1	1	1^{-+}	1^{+-}	2.3979	≈ 0
	$\chi_2^h(6^3P_2)$	1	1	2	2^{-+}	2^{-+}	2.4439	≈ 0
$1D$	$\eta_{c2}^h(1^1D_2)$	2	0	2	2^{++}	2^{--}	1.1156	≈ 0
	$\psi^h(1^3D_1)$	2	1	1	1^{+-}	1^{-+}	1.0905	≈ 0
	$\psi_2^h(1^3D_2)$	2	1	2	2^{+-}	2^{-+}	1.1133	≈ 0
	$\psi_3^h(1^3D_3)$	2	1	3	3^{+-}	3^{-+}	1.1262	≈ 0
$2D$	$\eta_{c2}^h(2^1D_2)$	2	0	2	2^{++}	2^{--}	1.4613	≈ 0
	$\psi^h(2^3D_1)$	2	1	1	1^{+-}	1^{-+}	1.4315	≈ 0
	$\psi_2^h(2^3D_2)$	2	1	2	2^{+-}	2^{-+}	1.4590	≈ 0
	$\psi_3^h(2^3D_3)$	2	1	3	3^{+-}	3^{-+}	1.4731	≈ 0

(Table continued)

TABLE VI. (*Continued*)

					J^{PC}		Our calculated $\sqrt{\langle r^2\rangle}$	Our calculated $\lvert R(0)\rvert^2$
n	Meson	L	S	J	$\varepsilon=1$	$\varepsilon=-1$	fm	Gev^3
$3D$	$\eta_{c2}^h(3^1D_2)$	2	0	2	2^{++}	2^{--}	1.7642	≈0
	$\psi^h(3^3D_1)$	2	1	1	1^{+-}	1^{-+}	1.7293	≈0
	$\psi_2^h(3^3D_2)$	2	1	2	2^{+-}	2^{-+}	1.7619	≈0
	$\psi_3^h(3^3D_3)$	2	1	3	3^{+-}	3^{-+}	1.777	≈0
$4D$	$\eta_{c2}^h(4^1D_2)$	2	0	2	2^{++}	2^{--}	2.0403	≈0
	$\psi^h(4^3D_1)$	2	1	1	1^{+-}	1^{-+}	1.9996	≈0
	$\psi_2^h(4^3D_2)$	2	1	2	2^{+-}	2^{-+}	2.0381	≈0
	$\psi_3^h(4^3D_3)$	2	1	3	3^{+-}	3^{-+}	2.0539	≈0
$5D$	$\eta_{c2}^h(5^1D_2)$	2	0	2	2^{++}	2^{--}	2.2974	≈0
	$\psi^h(5^3D_1)$	2	1	1	1^{+-}	1^{-+}	2.2502	≈0
	$\psi_2^h(5^3D_2)$	2	1	2	2^{+-}	2^{-+}	2.2953	≈0
	$\psi_3^h(5^3D_3)$	2	1	3	3^{+-}	3^{-+}	2.3117	≈0
$1F$	$h_{c3}^h(1^1F_3)$	3	0	3	3^{--}	3^{++}	1.2857	≈0
	$\chi_2^h(1^3F_2)$	3	1	2	2^{-+}	2^{+-}	1.2758	≈0
	$\chi_3^h(1^3F_3)$	3	1	3	3^{-+}	3^{+-}	1.2854	≈0
	$\chi_4^h(1^3F_4)$	3	1	4	4^{-+}	4^{+-}	1.2909	≈0
$2F$	$h_{c3}^h(2^1F_3)$	3	0	3	3^{--}	3^{++}	1.6110	≈0
	$\chi_2^h(2^3F_2)$	3	1	2	2^{-+}	2^{+-}	1.5997	≈0
	$\chi_3^h(2^3F_3)$	3	1	3	3^{-+}	3^{+-}	1.6105	≈0
	$\chi_4^h(2^3F_4)$	3	1	4	4^{-+}	4^{+-}	1.6171	≈0
$3F$	$h_{c3}^h(3^1F_3)$	3	0	3	3^{--}	3^{++}	1.9015	≈0
	$\chi_2^h(3^3F_2)$	3	1	2	2^{-+}	2^{+-}	1.8891	≈0
	$\chi_3^h(3^3F_3)$	3	1	3	3^{-+}	3^{+-}	1.9009	≈0
	$\chi_4^h(3^3F_4)$	3	1	4	4^{-+}	4^{+-}	1.9082	≈0
$4F$	$h_{c3}^h(4^1F_3)$	3	0	3	3^{--}	3^{++}	2.1688	≈0
	$\chi_2^h(4^3F_2)$	3	1	2	2^{-+}	2^{+-}	2.1556	≈0
	$\chi_3^h(4^3F_3)$	3	1	3	3^{-+}	3^{+-}	2.1681	≈0
	$\chi_4^h(4^3F_4)$	3	1	4	4^{-+}	4^{+-}	2.1761	≈0

coordinates to tame the potential at a small distance, as discussed in Ref. [66].

Above, the approach in which mass and state functions of charmonium states are calculated by using the effective quark-antiquark potential of Eq. (1) in the Schrödinger equation does not encompass the relativistic effects which are known to be significant for these states. To study the relativistic correction in charmonia, we apply the lowest-order relativistic correction to the Hamiltonian given by

$$\Delta H_{\rm rel} = -\left(\frac{1}{4m_c^3}\right)p^4. \tag{7}$$

Corresponding relativistic corrections to masses of charmonium states are calculated by using leading-order perturbation theory. Our results show that the relativistic corrections to the masses of charmonium states vary up to 7% when same values of parameters of the potential are used. However, when we refit the potential parameters to the masses of 11 experimentally known $c\bar{c}$ states, the difference between the relativistic and nonrelativistic results is significantly reduced. The best fit values of the potential parameters with relativistic correction are $\alpha_s = 0.480$, $b = 0.161$ GeV^2, $\sigma = 0.91$ GeV, and $m_c = 1.4670$ GeV, resulting in the values of the masses of charmonium states reported in the seventh column of Table I.

$E1$ radiative partial widths from meson to meson transitions are calculated by using the following expression mentioned in Ref. [65]:

$$\Gamma_{E1}(n^{2S+1}L_J \to n'^{2S'+1}L'_{J'} + \gamma) = \frac{4}{3}C_{fi}\delta_{SS'}e_c^2\alpha|\langle\psi_f|r|\psi_i\rangle|^2E_\gamma^3\frac{E_f^{(c\bar{c})}}{M_i^{(c\bar{c})}}. \tag{8}$$

TABLE VII. $S \to P\,E1$ radiative transitions. Experimental results are taken from Ref. [65]. The masses are taken from Tables I and II; we use the experimental masses if known. Otherwise, theoretically calculated masses are used.

			Our calculated Γ_{E1}				Our calculated Γ_{E1} for hybrid	
			NR	Relativistic	Other theoretically calculated Γ_{E1} [65] NR	Experimental Γ_{E1}	NR	Relativistic
Transition	Initial meson	Final meson	keV	keV	keV	keV	keV	keV
$2S \to 1P$	$\psi(2^3S_1)$	$\chi_2(1^3P_2)$	37.8723	35.503	38	27 ± 4	52.4875	53.9829
		$\chi_1(1^3P_1)$	54.221	50.9538	54	27 ± 3	35.8493	34.588
		$\chi_0(1^3P_0)$	62.5968	58.849	63	27 ± 3	18.0561	16.6958
	$\eta_c(2^1S_0)$	$h_c(1^1P_1)$	49.7831	45.1543	49		68.4258	71.3289
$3S \to 2P$	$\psi(3^3S_1)$	$\chi_2(2^3P_2)$	18.4517	4.044	14		82.6945	72.8367
		$\chi_1(2^3P_1)$	38.7222	17.0589	39		64.8613	55.0006
		$\chi_0(2^3P_0)$	53.4906	28.7006	54		37.5586	31.2277
	$\eta_c(3^1S_0)$	$h_c(2^1P_1)$	107.577	36.4002	105		119.603	107.831
$3S \to 1P$	$\psi(3^3S_1)$	$\chi_2(1^3P_2)$	0.541033	0.3013	0.70		0.0294	0.1222
		$\chi_1(1^3P_1)$	0.412865	0.2299	0.53		0.01836	0.0749
		$\chi_0(1^3P_0)$	0.213205	0.1187	0.27		0.007	0.0283
	$\eta_c(3^1S_0)$	$h_c(1^1P_1)$	10.7528	2.9957	9.1		3.4295	0.5424
$4S \to 3P$	$\psi(4^3S_1)$	$\chi_2(3^3P_2)$	84.9555	44.9699	68		102.849	77.8233
		$\chi_1(3^3P_1)$	126.866	91.3162	126		89.624	68.3772
		$\chi_0(3^3P_0)$	131.287	95.5685	0.003		57.4801	44.0157
	$\eta_c(4^1S_0)$	$h_c(3^1P_1)$	155.933	48.9384	159		164.542	130.49
$4S \to 2P$	$\psi(4^3S_1)$	$\chi_2(2^3P_2)$	0.65115	0.2513	0.62		0.11496	0.2588
		$\chi_1(2^3P_1)$	0.492438	0.1970	0.49		0.075	0.1669
		$\chi_0(2^3P_0)$	0.238085	0.0941	0.24		0.0302	0.0668
	$\eta_c(4^1S_0)$	$h_c(2^1P_1)$	10.1585	1.8977	10.1		4.288	0.2415
$4S \to 1P$	$\psi(4^3S_1)$	$\chi_2(^3P_2)$	0.605646	0.4225	0.61		0.0355	0.0078
		$\chi_1(^3P_1)$	0.412864	0.2880	0.41		0.0218	0.0048
		$\chi_0(^3P_0)$	0.175787	0.1226	0.18		0.0079	0.0017
	$\eta_c(4^1S_0)$	$h_c(^1P_1)$	5.05204	1.6698	5.2		2.2402	0.6377

Here, e_c, α, E_γ, $E_f^{c\bar{c}}$, and M_i stand for the charm quark charge, electromagnetic fine structure constant, final photon energy, total energy of the final state charmonium meson, and mass of initial state charmonium meson, respectively, and

$$C_{fi} = \max(L, L')(2J'+1)\begin{Bmatrix} L' & J' & S \\ J & L & 1 \end{Bmatrix}^2. \quad (9)$$

To calculate $M1$ radiative partial widths for meson to meson transitions, the following expression [65] is used:

$$\Gamma_{M1}(n^{2S+1}L_J \to n'^{2S'+1}L'_{J'} + \gamma) = \frac{4}{3}\frac{2J'+1}{2L+1}\delta_{LL'}\delta_{SS'\pm 1}e_c^2\frac{\alpha}{m_c^2}|\langle\psi_f|\psi_i\rangle|^2 E_\gamma^3\frac{E_f^{(c\bar{c})}}{M_i^{(c\bar{c})}}. \quad (10)$$

M_1 and E_1 transitions using relativistic and nonrelativistic masses are reported in Tables VII–XIV.

III. CHARACTERISTICS OF HYBRID CHARMONIUM MESONS

To describe hybrid mesons in a Born-Oppenheimer approximation, we used the static potential $V^h_{q\bar{q}}(r)$ in the place of $V_{q\bar{q}}(r)$ of Eq. (1):

$$V^h_{q\bar{q}}(r) = V_{q\bar{q}}(r) + V_g(r), \quad (11)$$

where $V_g(r)$ is the gluonic potential whose functional form varies with the level of gluonic excitation. This potential and the corresponding gluonic states are labeled by the magnitude ($\Lambda = 0, 1, 2, \ldots$ corresponding to greek letters $\Sigma, \Pi, \Delta, \ldots$) of the projection of the total angular momentum of gluons onto the quark-antiquark axis and the behavior of projection under the combined operation of charge conjugation and spatial inversion. The states which are even (odd) under this operation are represented by a subscript $\eta = g(u)$ on the label. However, the Σ states also

TABLE VIII. $1P$ and $2P$ $E1$ radiative transitions. Experimental results are particle data group [67] values from Ref. [74].

			Our calculated Γ_{E1}				Our calculated Γ_{E1} for hybrid	
			NR	Relativistic	Other theoretically calculated Γ_{E1} [65] NR	Experimental Γ_{E1}	NR	Relativistic
Transition	Initial meson	Final meson	keV	keV	keV	keV	keV	keV
$1P \to 1S$	$\chi_2(1^3P_2)$	$\psi(1^3S_1)$	424.525	437.584	424	380	76.2923	78.4537
	$\chi_1(1^3P_1)$		319.655	329.488	314	302	68.499	78.4537
	$\chi_0(1^3P_0)$		154.494	159.246	152	123	45.2691	52.0105
	$h_c(1^1P_1)$	$\eta_c(1^1S_0)$	490.328	570.53	498	372	89.8305	92.7853
$2P \to 2S$	$\chi_2(2^3P_2)$	$\psi_2(2^3S_1)$	287.543	377.091	304		114.688	112.158
	$\chi_1(2^3P_1)$		185.291	246.036	183		91.8365	93.2986
	$\chi_0(2^3P_0)$		65.337	108.31	64		49.8179	53.5944
	$h_c(2^1P_1)$	$\eta_c(2^1S_0)$	272.968	349.823	280		127.293	125.874
$2P \to 1S$	$\chi_2(2^3P_2)$	$\psi(1^3S_1)$	77.5048	70.9875	81		0.8872	0.4155
	$\chi_1(2^3P_1)$		68.7316	62.6288	71		0.8270	0.3923
	$\chi_0(2^3P_0)$		54.2844	50.9651	56		0.6939	0.3347
	$h_c(2^1P_1)$	$\eta_c(1^1S_0)$	141.861	114.078	140		7.9560	3.6517
$2P \to 1D$	$\chi_2(2^3P_2)$	$\psi_3(1^3D_3)$	78.693	60.6771	88		68.4722	65.7939
		$\psi_2(1^3D_2)$	15.3396	11.4779	17		10.949	9.8842
		$\psi(1^3D_1)$	1.67104	2.3056	1.9		0.7592	2.1752
	$\chi_1(2^3P_1)$	$\psi_2(1^3D_2)$	34.1414	21.7898	35		42.6113	40.0163
		$\psi(1^3D_1)$	21.5338	31.154	22		14.8266	47.4396
	$\chi_0(2^3P_0)$	$\psi(1^3D_1)$	13.5456	33.2356	13		29.6991	127.508
	$h_c(2^1P_1)$	$\eta_{2c}(1^1D_2)$	59.068	33.3607	60		63.8494	57.8128

require the sign of parity under reflection in the plane perpendicular to the quark-antiquark axis for their unique specification. The sign of this parity is put in the superscript of the state's label. In the present work, we study the hybrids in which the gluons are in the first excited state $\Lambda = 1$. This state is represented by the label Π_u. For hybrid mesons, the radial differential equation is given by

$$U''(r) + 2\mu\left(E - V^h_{q\bar{q}}(r) - \frac{\langle L^2_{q\bar{q}}\rangle}{2\mu r^2}\right)U(r) = 0, \qquad (12)$$

where the squared quark-antiquark angular momentum $\langle L^2_{q\bar{q}}\rangle$ [42,68] is given by

$$\langle L^2_{q\bar{q}}\rangle = L(L+1) - 2\Lambda^2 + \langle J^2_g\rangle. \qquad (13)$$

For the Π_u state, the squared gluon angular momentum $\langle J^2_g\rangle = 2$ and $\Lambda = 1$ [42], making $-2\Lambda^2 + \langle J^2_g\rangle = 0$. The parity and charge parity of the hybrid meson are given by

$$P = \epsilon(-1)^{L+\Lambda+1}, \qquad C = \epsilon\eta(-1)^{L+\Lambda+S}, \qquad (14)$$

where $\eta = -1$ and $\epsilon = \pm 1$ for the Π_u state [42]. In the present work, we use the following $V_g(r)$:

$$V_g(r) = \frac{c}{r} + A \times \exp^{-Br^{0.3723}}, \qquad (15)$$

where values of the constants $A = 3.4693$ GeV, $B = 1.0110$ GeV, and $c = 0.1745$ are fixed by our earlier fit [1] to the lattice data [42] of the parameters of the effective potential form corresponding to the Π_u gluonic state. It is shown in Ref. [1] that the form of Eq. (15) provides the best fit to the lattice data.

Using the hybrid potential of Eq. (11) for the Π_u gluonic state in Eq. (12), we calculated the masses, radial wave functions of the hybrid mesons, and hybrid to hybrid transitions by using the same technique as employed for conventional mesons (mentioned in Sec. II). The effect of relativistic correction is again determined using leading-order perturbation theory. The resultant wave functions are plotted in green lines in Figs. 1–4 corresponding to the same values of n, L, and S. These figures also show the comparison of the conventional and hybrid meson radial wave functions. The shape of these radial wave functions is not much affected by the addition of the V_g term for hybrids, although the values of masses are significantly increased for the same values of n, L, and S.

TABLE IX. $3P$ $E1$ radiative transitions.

			Our calculated Γ_{E1}			Our calculated Γ_{E1} for hybrid	
			NR	Relativistic	Other theoretically calculated Γ_{E1} [65] NR	NR	Relativistic
Transition	Initial meson	Final meson	keV	keV	keV	keV	keV
$3P \to 3S$	$\chi_2(3^3P_2)$	$\psi(3^3S_1)$	469.74	552.378	509	146.323	138.537
	$\chi_1(3^3P_1)$		301.752	339.862	303	107.286	102.956
	$\chi_0(3^3P_0)$		108.078	140.784	109	48.8432	49.4522
	$h_c(3^1P_1)$	$\eta_c(3^1S_0)$	276.451	358.257	276	152.437	143.525
$3P \to 2S$	$\chi_2(3^3P_2)$	$\psi(2^3S_1)$	52.9422	48.2333	55	2.165	1.3547
	$\chi_1(3^3P_1)$		44.5896	39.6913	45	1.9595	1.2312
	$\chi_0(3^3P_0)$		31.7371	29.2243	32	1.5683	0.9985
	$h_c(3^1P_1)$	$\eta_c(2^1S_0)$	74.7089	58.3516	75	11.8614	5.7040
$3P \to 1S$	$\chi_2(3^3P_2)$	$\psi(1^3S_1)$	33.4109	27.2067	34	0.2066	0.0512
	$\chi_1(3^3P_1)$		30.855	24.8275	31	0.1955	0.0486
	$\chi_0(3^3P_0)$		26.5634	21.6538	27	0.1733	0.0434
	$h_c(3^1P_1)$	$\eta_c(1^1S_0)$	72.122	47.532	72	4.1948	1.4827
$3P \to 2D$	$\chi_2(3^3P_2)$	$\psi_3(2^3D_3)$	131.185	95.098	148	119.852	106.399
		$\psi_2(2^3D_2)$	27.0618	20.3685	31	20.4455	17.3847
		$\psi_(2^3D_1)$	1.7764	2.29	2.1	1.5084	5.3930
	$\chi_1(3^3P_1)$	$\psi_2(2^3D_2)$	57.0882	32.9113	58	72.2218	61.7364
		$\psi(2^3D_1)$	18.6351	23.1234	19	26.9846	111.051
	$\chi_0(3^3P_0)$	$\psi(2^3D_1)$	4.3348	10.7876	4.4	45.563	283.267
	$h_c(3^1P_1)$	$\eta_{2c}(2^1D_2)$	100.263	52.3298	99	109.704	89.8848
$3P \to 1D$	$\chi_2(3^3P_2)$	$\psi_3(1^3D_3)$	0.0476	0.0939	0.049	0.3713	0.440
		$\psi_2(1^3D_2)$	0.0087	0.0170	0.0091	0.0639	0.0742
		$\psi_(1^3D_1)$	0.0007	0.0016	0.0007	0.0043	0.0077
	$\chi_1(3^3P_1)$	$\psi_2(1^3D_2)$	0.0351	0.0652	0.035	0.2880	0.3354
		$\psi(1^3D_1)$	0.0139	0.0326	0.014	0.0973	0.1773
	$\chi_0(3^3P_0)$	$\psi(1^3D_1)$	0.0369	0.0906	0.037	0.3086	0.590
	$h_c(3^1P_1)$	$\eta_{2c}(1^1D_2)$	0.1618	0.0161	0.16	0.1555	0.4574

IV. RESULTS AND CONCLUSIONS

In previous work [1], we calculated masses, root mean square radii, and radial wave functions of 0^{+-}, 1^{-+}, and 2^{+-} J^{PC} states of the conventional and hybrid charmonium mesons. Now, considering the expected phenomenological challenges in the foreseeable future, we have extended this work [1] by calculating these properties for a rather comprehensive spectrum of conventional and hybrid charmonium mesons. We do this by including the radially excited J^{PC} states not addressed in the previous study. In Table I, our calculated masses are reported for the ground and radially excited states of charmonium mesons with and without relativistic correction along with the experimental and theoretical predictions of the others' works. Our calculated masses with NR potential agree with the masses reported in Refs. [65,69] as well as the experimental values. In Table II, the calculated masses of hybrid charmonium mesons are reported for same values of n, L, and S as used for the conventional mesons. In order to distinguish the hybrids from nonhybrids, we suggest and use here a workable notation of using a superscript h to the symbol of the conventional meson with the same n, L, and S. These results show that for the same quantum numbers (n, L, and S), the mass of a hybrid meson is significantly greater than the corresponding conventional meson. It is noted that the J^{PC} of each hybrid meson is also different from the corresponding conventional meson for same L and S. This difference arises from the effect of the angular momentum of the gluonic field which contributes in the former case. It is also noted that the gluonic potential Π_u applied in this work allows two possible values of ε in Eq. (14). As a result, we obtain two degenerate hybrid states with opposite values of P and C. All the hybrids corresponding to $\varepsilon = 1$ are nonexotic, whereas exotic hybrid mesons are obtained for $\varepsilon = -1$, as shown in Table II. We find that the lightest hybrid charmonium state has mass 4.0802 GeV and $J^{PC} = 0^{++}(0^{--})$. This result can be compared with the result reported in Refs. [20,23] that use the flux-tube model to predict that the lowest state charmonium hybrid meson mass is approximately 4.2 GeV. The similar result for the lowest state hybrid charmonium meson's mass (4.09 GeV) is predicted in Ref. [70] by using a linear plus Coulombic potential model.

TABLE X. $1D$ and $2D$ $E1$ radiative transitions. Experimental results are taken from Ref. [65].

			Our calculated Γ_{E1}				Our calculated Γ_{E1} for hybrid	
			NR	Relativistic	Other theoretically calculated Γ_{E1} [65] NR	Experimental Γ_{E1}	NR	Relativistic
Transition	Initial meson	Final meson	keV	keV	keV	keV	keV	keV
$1D \to 1P$	$\psi_3(1^3D_3)$	$\chi_2(1^3P_2)$	271.137	397.684	272		109.039	112.974
	$\psi_2(1^3D_2)$	$\chi_2(1^3P_2)$	64.0588	96.5234	64		30.3117	33.1196
		$\chi_1(1^3P_1)$	311.2	438.159	307		102.035	105.255
	$\psi(1^3D_1)$	$\chi_2(1^3P_2)$	4.8627	4.7324	4.9	≤ 330	3.2460	0.6597
		$\chi_1(1^3P_1)$	126.216	122.833	125	280 ± 100	54.7141	10.9821
		$\chi_0(1^3P_0)$	405.431	394.563	403	320 ± 120	106.125	25.7501
	$h_{c2}(1^1D_2)$	$h_c(1^1P_1)$	341.51	480.201	339		127.525	134.244
$2D \to 2P$	$\psi_3(2^3D_3)$	$\chi_2(2^3P_2)$	260.381	253.36	239		127.036	119.494
	$\psi_2(2^3D_2)$	$\chi_2(2^3P_2)$	58.4946	55.9308	52		33.2531	32.5774
		$\chi_1(2^3P_1)$	300.632	299.34	298		126.725	119.332
	$\psi(2^3D_1)$	$\chi_2(2^3P_2)$	6.5773	3.9667	5.9		3.33	0.1503
		$\chi_1(2^3P_1)$	168.664	116.186	168		63.9937	3.9456
		$\chi_0(2^3P_0)$	483.705	339.764	483		142.889	15.9789
	$\eta_{c2}(2^1D_2)$	$h_c(2^1P_1)$	338.241	363.001	336		154.573	203.189
$2D \to 1P$	$\psi_3(2^3D_3)$	$\chi_2(1^3P_2)$	28.8837	26.5225	29		0.6039	0.4675
	$\psi_2(2^3D_2)$	$\chi_2(1^3P_2)$	6.9917	6.3982	7.1		0.1531	0.1199
		$\chi_1(1^3P_1)$	25.3652	22.9949	26		0.4776	0.3671
	$\psi(2^3D_1)$	$\chi_2(1^3P_2)$	0.7769	06305	0.79		0.01649	0.0069
		$\chi_1(1^3P_1)$	14.0918	11.4338	14		0.2574	0.1069
		$\chi_0(1^3P_0)$	26.7675	21.7083	27		0.3927	0.1659
	$h_{c2}(2^1D_2)$	$h_c(1^1P_1)$	39.6531	35.3936	40		0.996	0.8504
$2D \to 1F$	$\psi_3(2^3D_3)$	$\chi_4(1^3F_4)$	63.7077	47.7232	66		58.2025	52.6007
	$\psi_2(2^3D_2)$	$\chi_3(1^3F_3)$	4.7124	3.099	4.8		3.9086	3.1857
		$\chi_2(1^3F_2)$	0.1338	0.0790	14		0.0978	0.0729
	$\psi(2^3D_1)$	$\chi_3(1^3F_3)$	44.9644	28.0715	49		45.9766	39.3028
		$\chi_2(1^3F_2)$	5.5826	3.1069	5.6		5.0455	3.9641
	$\psi(2^3D_1)$	$\chi_2(1^3F_2)$	51.1584	11.7495	51		40.4282	0.3548
	$\eta_{c2}(2^1D_2)$	$h_{c3}(1^1F_3)$	53.858	32.1154	54		53.661	45.3408

By comparing the experimental masses of various X, Y, and Z particles with our calculated masses (with relativistic correction) having the same J^{PC}, we suggest assigning the states calculated by us to the experimentally observed particles, as in Table III. These results can help in experimentally recognizing hybrid mesons. In Table IV, we present the comparison of our results with other theoretical studies of hybrid charmonium states in the

TABLE XI. $1F$ $E1$ radiative transitions.

			Our calculated Γ_{E1}			Our calculated Γ_{E1} for hybrid	
			NR	Relativistic	Other theoretically calculated Γ_{E1} [65] NR	NR	Relativistic
Transition	Initial meson	Final meson	keV	keV	keV	keV	keV
$1F \to 1D$	$\chi_4(1^3F_4)$	$\psi_3(1^3D_3)$	337.608	326.749	332	159.057	158.787
	$\chi_3(1^3F_3)$	$\psi_3(1^3D_3)$	41.3732	42.6351	41	22.0405	23.625
		$\psi_2(1^3D_2)$	352.155	353.95	354	158.869	161.494
	$\chi_2(1^3F_2)$	$\psi_3(1^3D_3)$	1.8052	1.7157	1.6	0.9768	1.1008
		$\psi_2(1^3D_2)$	61.8594	65.5198	62	30.9184	33.1997
		$\psi(1^3D_1)$	477.097	744.19	475	173.038	512.603
	$h_{c3}(1^1F_3)$	$\eta_{c2}(1^1D_2)$	384.4	393.26	387	176.469	181.051

TABLE XII. $2F$ $E1$ radiative transitions.

			Our calculated Γ_{E1}			Our calculated Γ_{E1} for hybrid	
			NR	Relativistic	Other theoretically calculated Γ_{E1} [65] NR	NR	Relativistic
Transition	Initial meson	Final meson	keV	keV	keV	keV	keV
$2F \to 2D$	$\chi_4(2^3F_4)$	$\psi_3(2^3D_3)$	313.328	278.883	307	173.845	156.358
	$\chi_3(2^3F_3)$	$\psi_3(2^3D_3)$	37.4222	35.7473	36	23.2673	22.6508
		$\psi_2(2^3D_2)$	334.441	325.15	334	178.07	166.682
	$\chi_2(2^3F_2)$	$\psi_3(2^3D_3)$	1.45777	1.4746	1.4	0.9965	1.0266
		$\psi(2^3D_2)$	57.0568	58.601	58	33.401	33.1715
		$\psi(2^3D_1)$	304.421	461.5	306	198.523	736.075
	$h_{c3}(2^1F_3)$	$\eta_{c2}(2^1D_2)$	364.027	363.36	362	196.08	185.655
$2F \to 1D$	$\chi_4(2^3F_4)$	$\psi_3(1^3D_3)$	19.9012	15.4547	20	0.9449	0.8467
	$\chi_3(2^3F_3)$	$\psi_3(1^3D_3)$	2.26255	1.7979	2.3	0.1113	0.1022
		$\psi_2(1^3D_2)$	18.537	14.599	19	0.8586	0.7725
	$\chi_2(2^3F_2)$	$\psi_3(1^3D_3)$	0.08974	0.0726	0.090	0.0045	0.0042
		$\psi(1^3D_2)$	3.21694	2.5806	3.2	0.1536	0.1409
		$\psi(1^3D_1)$	20.0554	19.332	20	0.8402	1.1696
	$h_{c3}(2^1F_3)$	$\eta_{c2}(1^1D_2)$	21.5771	17.4017	22	1.0093	0.9412
$2F \to 1G$	$\chi_4(2^3F_4)$	$\psi_5(1^3G_5)$	53.8555	32.7248	54		
		$\psi_4(1^3G_4)$	1.99134	0.9993	2.0		
		$\psi_3(1^3G_3)$	0.02559	0.0105	0.025		
	$\chi_3(2^3F_3)$	$\psi_4(1^3G_4)$	42.9011	25.0232	43		
		$\psi_3(1^3G_3)$	2.33494	1.1459	2.3		
	$\chi_2(2^3F_2)$	$\psi_3(1^3G_3)$	35.7719	19.5170	36		
	$h_{c3}(2^1F_3)$	$\eta_{c4}(1^1G_4)$	47.1095	27.1812	47		

flux-tube model, the constituent glue model, and the lattice QCD. Root mean square radii and radial wave functions at the origin for the ground and radially excited states of conventional and hybrid charmonium mesons are reported in Tables V and VI, respectively. These results show that with the same quantum numbers (n, L, and S), root mean square radii of hybrid mesons are greater than those for conventional mesons. It is also noted that, similar to the conventional mesons case, radii of hybrid mesons increase with radial and angular excitations. Tables IV and V show that $|R(0)|^2$ is nonzero only for S states and decreases with the radial excitation. As scalar form factors [57], energy shifts, and polarizabilities [59] depend on the root mean square radii, we predict a significant change in the values of these quantities for a hybrid meson as compared to those for the corresponding conventional meson for the same quantum numbers. Thus, it is highly interesting to compare our results with experimental findings of conventional and exotic mesons. In Tables VII–XIV, M_1 and E_1 radiative partial widths are reported. In the second and

TABLE XIII. $1G$ $E1$ radiative transitions.

			Our calculated Γ_{E1}		
			NR	Relativistic	Other theoretically calculated Γ_{E1} [65] NR
Transition	Initial meson	Final meson	keV	keV	keV
$1G \to 1F$	$\psi_5(1^3G_5)$	$\chi_4(1^3F_4)$	373.583	373.335	373
	$\psi_4(1^3G_4)$	$\chi_4(1^3F_4)$	28.5777	30.2781	29
		$\chi_3(1^3F_3)$	385.47	382.394	382
	$\psi_3(1^3G_3)$	$\chi_4(1^3F_4)$	0.65313	0.7286	0.66
		$\chi_3(1^3F_3)$	37.1617	39.0477	37
		$\chi_2(1^3F_2)$	422.944	419.428	425
	$\eta_{c4}(1^1G_4)$	$h_{c3}(1^1F_3)$	408.624	406.979	407

TABLE XIV. $M1$ radiative transitions. Experimental results are particle data group results [67] from Ref. [74]. One exception is the $\eta_c 3^1S_0$; for the NR case, we assume a mass of 4.0115 GeV [the difference of the mass of known $\psi(4040)$ and the theoretical $3S$ splitting]. In the relativistic case, $\eta_c 3^1S_0 = 4.0294$ GeV.

			Our calculated Γ_{M1}				Our calculated Γ_{M1} for hybrid	
			NR	Relativistic	Other theoretically calculated Γ_{M1} [65] NR	Experimental Γ_{M1}	NR	Relativistic
Transition	Initial meson	Final meson	keV	keV	keV	keV	keV	keV
$1S$	$J/\psi(1^3S_1)$	$\eta_c(1^1S_0)$	2.75188	2.7654	2.9	1.5	0.03398	0.0240
$2S$	$\psi(2^3S_1)$	$\eta_c(2^1S_0)$	0.196844	0.1980	0.21		0.0387	0.0282
		$\eta_c(1^1S_0)$	4.53183	3.3698	4.6	0.8 ± 0.2	0.619	0.2965
	$\eta_c(2^1S_0)$	$j/\psi(1^3S_1)$	7.96173	5.7919	7.9		1.3094	0.6273
$3S$	$\psi(3^3S_1)$	$\eta_c(3^1S_0)$	0.044139	0.0023	0.046		0.0262	0.0222
		$\eta_c(2^1S_0)$	0.6075	0.4702	0.61		0.2872	0.1225
		$\eta_c(1^1S_0)$	3.48334	2.4944	3.5		0.9238	0.3722
	$\eta_c(3^1S_0)$	$\psi(2^3S_1)$	1.32214	1.1424	1.3		0.6669	0.2664
		$J/\psi(1^3S_1)$	6.27928	4.7885	6.3		1.8697	0.7989
$2P$	$h_c(2^1P_1)$	$\chi_2(1^3P_2)$	0.070438	0.0589	0.071		0.0318	0.0299
		$\chi_1(1^3P_1)$	0.05772	0.0476	0.058		0.0203	0.0185
		$\chi_0(1^3P_0)$	0.03335	0.0269	0.033		0.0083	0.0074
	$\chi_2(2^3P_2)$	$h_c(1^1P_1)$	0.0604237	0.0537	0.067		0.0211	0.0202
	$\chi_1(2^3P_1)$	$h_c(1^1P_1)$	0.0464833	0.0412	0.51		0.0188	0.0185
	$\chi_0(2^3P_0)$	$h_c(1^1P_1)$	0.0265996	0.0258	0.029		0.0141	0.0142

third columns of these tables, the initial and final states of charmonium mesons are written. In the last two columns of Tables VII–XIV, radiative widths are reported for the transitions from hybrid to hybrid charmonium meson states. The initial and final transition states of the hybrid mesons have the symbols reported in the second and third columns with the addition of h in the superscript.

ACKNOWLEDGMENTS

B. M. and F. A. acknowledge the financial support of Punjab University for the Projects (Sr. 215 PU Project 2012-13 and Sr. 220 PU Project 2012-13). N. A. and B. M. are grateful to the Higher Education Commission of Pakistan for their financial support (No. PM-IPFP/HRD/HEC/2012/4026).

[1] N. Akbar, B. Masud, and S. Noor, Eur. Phys. J. A **47**, 124 (2011); N. Akbar, B. Masud, and S. Noor, Eur. Phys. J. A **50**, 121 (2014).
[2] T. Barnes, arXiv:hep-ph/0103142.
[3] M. Moinester, arXiv:hep-ex/0012063; M. Moinester, arXiv:hep-ex/0003008.
[4] S. Godfrey, arXiv:hep-ph/0211464; B. Grube (for the COMPASS Collaboration), in *Proceedings of the "Xth Quark Confinement and the Hadron Spectrum" (ConfX), TUM Campus Garching, Munich, Germany, 2012* (Sissa, Trieste, 2013).
[5] F. E. Close and P. R. Page, Phys. Lett. B **628**, 215 (2005); T. Uglov, arXiv:1011.3369v1.
[6] D. S. Carman, J. Phys. Conf. Ser. **69**, 012011 (2007).
[7] GlueX Collaboration, Report No. GLUEX-DOC-1962; Report No. JLAB-PHY-12-1632; arXiv:1210.4508; arXiv:1305.1523.
[8] D. Asner (for the CLEO Collaboration), AIP Conf. Proc. **722**, 82 (2004).
[9] K.-T. Brinkmann, P. Gianotti, and I. Lehmann, Nucl. Phys. News **16**, 15 (2006); J. G. Messchendorp (for the PANDA Collaboration), arXiv:1001.0272.
[10] M. Yu. Barabanov, A. S. Vodopyanov, V. Kh. Dodokhov, and V. A. Babkin, arXiv:1108.5847v1.
[11] U. Wiedner, Prog. Part. Nucl. Phys. **66**, 477 (2011).
[12] M. Alekseev *et al.* (COMPASS Collaboration), Phys. Rev. Lett. **104**, 241803 (2010); B. Grube *et al.* (COMPASS Collaboration), Eur. Phys. J. Web Conf. **3**, 07018 (2010).
[13] M. Lu *et al.* (E852 Collaboration), Phys. Rev. Lett. **94**, 032002 (2005).
[14] G. J. Ding and M. L. Yan, Phys. Lett. B **650**, 390 (2007).
[15] S. L. Zhu, Phys. Lett. B **625**, 212 (2005); E. Kou and O. Pene, Phys. Lett. B **631**, 164 (2005).
[16] F. Iddir and L. Semlala, arXiv:hep-ph/0611183v3.
[17] S. Godfrey, in *Proceedings of the Flavour Physics and CP Violation Conference, Vancouver, 2006*, eConf C060409,

015 (2006); S. Godfrey and S. L. Olsen, Annu. Rev. Nucl. Part. Sci. **58**, 51 (2008); S. Godfrey, arXiv:0910.3409v2.
[18] C. Z. Yuan *et al.* (Belle Collaboration), arXiv:0910.3138.
[19] N. Isgur and J. Paton, Phys. Lett. **124B**, 247 (1983).
[20] N. Isgur and J. Paton, Phys. Rev. D **31**, 2910 (1985).
[21] N. Isgur, R. Kokosky, and J. Paton, Phys. Rev. Lett. **54**, 869 (1985).
[22] F. E. Close and P. R. Page, Nucl. Phys. **B443**, 233 (1995); Phys. Rev. D **52**, 1706 (1995).
[23] T. Barnes, F. E. Close, and E. S. Swanson, Phys. Rev. D **52**, 5242 (1995).
[24] E. S. Swanson, arXiv:hep-ph/0311328.
[25] Yu. S. Kalashnikova and A. V. Nefediev, Phys. Rev. D **77**, 054025 (2008).
[26] C. Semay, F. Buisseret, and B. Silvestre-Brac, Phys. Rev. D **79**, 094020 (2009).
[27] E. S. Swanson and A. P. Szczepaniak, Phys. Rev. D **59**, 014035 (1998).
[28] F. Iddir, S. Safir, and O. Pène, Phys. Lett. B **433**, 125 (1998); F. Iddir and L. Semlala, arXiv:hep-ph/0211289; arXiv:hep-ph/0611165; L. Semlala and F. Iddir, Int. J. Mod. Phys. A **23**, 5229 (2008).
[29] Yu. B. Yufryakov, arXiv:hep-ph/9510358.
[30] C. McNeile and C. Michael, Phys. Rev. D **73**, 074506 (2006).
[31] Y. Liu and X. Q. Luo, Phys. Rev. D **73**, 054510 (2006).
[32] L. Liu, G. Moira, M. Peardona, S. M. Ryana, C. E. Thomasa, P. Vilasecaa, J. J. Dudekb, R. G. Edwards, B. J. David, and G. Richards, J. High Energy Phys. 07 (2012) 126.
[33] G. Moir, M. Peardon, S. M. Ryan, C. E. Thomas, and L. Liu, arXiv:1312.1361v1.
[34] C. Bernard, T. Burch, C. DeTar, S. Gottlieb, E. B. Gregory, U. M. Heller, J. Osborn, R. Sugar, and D. Toussaint, Nucl. Phys. B, Proc. Suppl. **119**, 260 (2003).
[35] X. Q. Luo and Z. H. Mei, Nucl. Phys. B, Proc. Suppl. **119**, 263 (2003).
[36] T. W. Chiu and T. H. Hsieh, Phys. Rev. D **73**, 094510 (2006).
[37] X. Q. Luo and Y. Liu, Phys. Rev. D **74**, 034502 (2006); **74**, 039902 (2006).
[38] G. S. Bali, Int. J. Mod. Phys. A **21**, 5610 (2006).
[39] K. J. Juge, A. O. Cais, M. B. Oktay, M. J. Peadon, S. M. Ryan, and J. I. Skullerud, *Proc. Sci.*, LAT2006 (2006) 193.
[40] J. J. Dudek and E. Rrapaj, Phys. Rev. D **78**, 094504 (2008).
[41] P. Lacock, C. Michael, P. Boyle, and P. Rowland, Phys. Lett. B **401**, 308 (1997).
[42] K. J. Juge, J. Kuti, and C. J. Morningstar, Nucl. Phys. B, Proc. Suppl. **63**, 326 (1998).
[43] S. Prelovsek, arXiv:1310.4354v2.
[44] R. Berg, D. Harnett, R. T. Kleiv, and T. G. Steele, Phys. Rev. D **86**, 034002 (2012).
[45] D. Harnett, R. T. Kleiv, T. G. Steele, and H.-y. Jin, J. Phys. G **39**, 125003 (2012).
[46] H. Y. Jin, J. G. Korner, and T. G. Steele, Phys. Rev. D **67**, 014025 (2003).
[47] C. F. Qiao, L. Tang, G. Hao, and X. Q. Li, J. Phys. G **39**, 015005 (2012).
[48] R. T. Kleiv, D. Harnett, T. G. Steele, and H.-y. Jin, Nucl. Phys. B, Proc. Suppl. **234**, 150 (2013).
[49] W. Chen, R. T. Kleiv, T. G. Steele, B. Bulthuis, D. Harnett, J. Ho, T. Richards, and S.-L. Zhu, J. High Energy Phys. 09 (2013) 019.
[50] I. J. General, S. R. Cotanch, and F. J. Llanes-Estrada, Eur. Phys. J. C **51**, 347 (2007).
[51] S. R. Cotanch, I. J. General, and P. Wang, Eur. Phys. J. A **31**, 656 (2007).
[52] S. R. Cotanch and F. J. Llanes-Estrada, Phys. Lett. B **504**, 15 (2001).
[53] K. J. Juge, J. Kuti, and C. J. Morningstar, Nucl. Phys. B, Proc. Suppl. **83–84**, 304 (2000).
[54] E. Braaten, C. Langmack, and D. H. Smith, Phys. Rev. D **90**, 014044 (2014).
[55] P. Guo, A. P. Szczepaniak, G. Galata, A. Vassallo, and E. Santopinto, Phys. Rev. D **78**, 056003 (2008).
[56] B. Ketzer, *Proc. Sci.*, QNP2012 (2012) 025 [arXiv:1208.5125].
[57] B. Ananthanarayan, I. Caprini, G. Colangelo, J. Gasser, and H. Leutwyler, Phys. Lett. B **602**, 218 (2004).
[58] K. L. Haglin, in *Proceedings of the 18th Winter Workshop on Nuclear Dynamics, Nassau, Bahamas, 2002* (EP Sytema, Debrecen, 2002).
[59] S. I. Kruglov, Phys. Rev. D **60**, 116009 (1999).
[60] H.-b. Wang and Y.-P. Yao, Phys. Rev. D **70**, 094046 (2004).
[61] B. Patel and P. C. Vinodkumar, J. Phys. G **36**, 035003 (2009) and references therein.
[62] H.-W. Ke, X.-Q. Li, Z.-T. Wei, and X. Liu, Phys. Rev. D **82**, 034023 (2010).
[63] E. J. Eichten and C. Quigg, Phys. Rev. D **52**, 1726 (1995).
[64] C. H. Chaug, C. F. Qiao, and J. X. Wang, Phys. Rev. D **57**, 4035 (1998).
[65] T. Barnes, S. Godfrey, and E. S. Swanson, Phys. Rev. D **72**, 054026 (2005).
[66] S. Godfrey and N. Isgur, Phys. Rev. D **32**, 189 (1985).
[67] J. Beringer *et al.* (Particle Data Group), Phys. Rev. D **86**, 010001 (2012).
[68] K. J. Juge, J. Kuti, and C. J. Morningstar, Phys. Rev. Lett. **82**, 4400 (1999).
[69] D. Ebert, R. N. Faustov, and V. O. Galkin, Eur. Phys. J. C **71**, 1825 (2011).
[70] F. Iddir and L. Semlala, arXiv:hep-ph/0211289v3.
[71] G. T. Bodwin, E. Braaten, E. Eichten, S. L. Olsen, T. K. Pedlar, and J. Russ, arXiv:1307.7425 and references therein.
[72] L. Liu, S. M. Ryan, M. Peardon, G. Moir, and P. Vilaseca, *Proc. Sci.*, LATTICE2011 (2011) 140.
[73] C.-Y. Wong, E. S. Swanson, and T. Barnes, Phys. Rev. C **65**, 014903 (2001).
[74] P. Guo, T. Yepez-Martinez, and A. P. Szczepaniak, Phys. Rev. D **89**, 116005 (2014).